Babes – Bolyai University
Faculty of Chemistry and Chemical Engineering

PhD THESIS

- Summary -

Catalytic reduction of nitrogen oxides from the residual gases of the ^{15}N separation column

PhD Student
Eng. Maria Cîmpean (married Miheţ)

Scientific Advisor
Prof. Dr. Eng. Paul Şerban Agachi

Cluj-Napoca
2015

JURY:

PRESIDENT:	**Prof. Dr. Eng. PETRU ILEA** *Babeş-Bolyai University,* *Faculty of Chemistry and Chemical Engineering*
COORDINATOR:	**Prof. Dr. Eng. PAUL-ŞERBAN AGACHI** *Babeş-Bolyai University,* *Faculty of Chemistry and Chemical Engineering*
REVIEWERS:	**Prof. Dr. Eng. GRIGORE BOZGA** *University Politehnica of Bucharest,* *Faculty of Applied Chemistry and Material Science*
	Assoc. Prof. Dr. RODICA ZĂVOIANU *University of Bucharest, Faculty of Chemistry*
	Prof. Dr. Eng. VASILE-MIRCEA CRISTEA *Babeş-Bolyai University,* *Faculty of Chemistry and Chemical Engineering*

Acknowledgements

I would like to thank God for the privilege I had to bring to an end what I started years ago, as he completed my health and renewed my power for work. Without his help and blessing this would not have been possible.

Also, I am grateful for all those who had a good word for me during this time, an advice, or even some criticism. All these made me go ahead and not give in. I am mostly thankful for Prof. Dr. Eng. Paul-Şerban Agachi, from whom I received liberty in action and understanding when I mostly needed it.

I am delighted and thankful to God for the place where I was allowed to pursue my research in the field of the thesis, and other domains also, the National Institute for Research and Development for Isotopic and Molecular Technologies-INCDTIM, Cluj-Napoca, and, also, for the financial support I received in this endeavor through the favor of Director Dr. Eng. Adrian Bot. Also, I am grateful for the freedom I enjoyed these years in learning to work with various equipments in our laboratory, through the incentive of Dr. Eng. Valer Almăşan. Furthermore, I am grateful for the equilibrium I found in my colleague and friend, Dr. Mihaela Diana Lazăr, through all the discussions and debates in which she helped me see the big picture, and not only every single detail.

I am also grateful for Prof. Dr. Eng. Vasile-Mircea Cristea, who guided me starting with my bachelor years. All the discussions and his availability are appreciated.

Last, but not least, I feel truly blessed to have such a family, to enjoy the comfort and serenity I can find in it. My family carried the burden all these years together with me, but mostly, Timi, my husband. For you all I am especially grateful to God.

CONTENTS OF THE THESIS

The thesis was originally written in English.

NOTE: Numbers of references, figures, tables, and equations are identical to those in the thesis.

INTRODUCTION

Environmental protection in general and abatement of gaseous pollutants in particular are of great concern for both authorities and researchers. Important financial and research effort has been dedicated in the last decades in order to minimize the harmful environmental impact of pollutants resulted as a consequence of the growing technological and industrial development. Most of the industrial or automotive processes give rise to exhaust gases with various noxious components such as: carbon monoxide (CO), carbon dioxide (CO_2), volatile organic compounds (VOCs), nitrogen oxides (NOx), sulphur oxides (SOx), particulate matter (PM), etc. However, the characteristics of these exhaust gases are diverse, mostly regarding their composition and temperature, so that abatement technologies must be adapted to the specifics of the process of interest.

The ***aim of this thesis*** is to provide an efficient solution for the abatement of nitrogen oxides resulted as exhaust gases in the ^{15}N separation plant, at INCDTIM in Cluj–Napoca. Separation of ^{15}N isotope is performed by NO–HNO_3 isotopic exchange in a plant consisting in two separation columns, and several other units, as described in detail in the work of Axente et al. [1]. Compared to other exhaust gases containing nitrogen oxides as environmental harmful pollutants, in this particular case the concentration of NOx is significantly higher (up to 2 %), the other major component being nitrogen. One very important characteristic is that these exhaust gases contain very low amounts of oxygen or other components (e.g. SO_2), so that these exhaust gases can be assimilated to a model gaseous mixture of NOx in an inert gas, such as N_2 or Ar. "Efficient" removal of NOx involves two important aspects: (i) use of catalysts with good catalytic performance in the reduction by H_2 of NOx (high conversion, very good N_2 selectivities, and good stability in time), but with low production costs due to raw materials or synthesis method, and (ii) reduction of NOx at reaction temperatures as low as possible, considering that the exhaust gases resulted in the ^{15}N separation plant are cold (~26°C).

The ***specific objectives*** resulted from this general scope are: (1) design, synthesis, characterization and testing of catalysts, as inexpensive as possible, for the efficient removal of NOx by catalytic reduction with hydrogen as reducing agent at low reaction temperatures, and (2) mathematical modeling of the catalytic reactor used in the deNOx process based on the developed catalysts.

In respect to the **first objective**, design of efficient, but inexpensive catalytic materials was targeted. Thus, starting with monometallic noble metal catalysts, with alumina as supporting material, the efficiency of NOx removal by hydrogen was tested and the best reaction conditions were determined. These reaction conditions were further used to test the catalytic activity of cheaper bimetallic Ni based catalysts: Ni–Pt/Al_2O_3, Ni–Pd/Al_2O_3, and Ni–Rh/Al_2O_3. Regarding the **second objective**, a mathematical model of the deNOx reactor was developed, considering a fixed catalytic bed formed by granular catalyst. The reactor model was simulated using COMSOL Multiphysics and MATLAB. The developed reactor model was used for parametric studies in order to study the influence of several parameters upon the catalytic performance (temperature influence, effect of *GHSV*, influence of NO concentration in the feed, effect of reactants ratio, NO/H_2, etc).

The thesis is structured in six chapters. The *first chapter* provides an overview upon the issues related to nitrogen oxides pollutants, addressing their source and environmental impact, as well as the technologies used up to now for their abatement. *Chapter 2* describes in detail the methods used for the preparation of the mono– and bimetallic catalysts, the techniques employed for the physico–chemical characterization of the catalytic materials, as well as the experimental methods developed for the assessment of the catalytic activity. *Chapters 3 and 4* present the research results regarding the development of efficient catalysts for the reduction of NOx by H_2 (*objective 1*), with detailed discussions on the catalytic performance in relation with catalysts' characteristics obtained from catalysts' characterization. *Chapter 5* presents the mathematical model developed for the catalytic deNOx reactor, with the corresponding simulation results, as well as parametric studies performed by means of this model (*objective 2*). The *final chapter* presents the general conclusions of this work and some future perspectives.

Keywords: nitrogen oxides, noble metal (1wt.%)/alumina catalyst, Ni (10wt.%)–noble metal (0.5wt.%)/alumina catalyst, H_2–TPD, NO–TPD, plug flow reactor, mathematical model, parametric study.

CHAPTER 1

State of the art in the abatement of nitrogen oxides (NOx): Literature Survey

The aim of this chapter is to provide a scientific background for the NOx problem: formation mechanisms, sources and environmental impact of NOx emissions. Some regulatory aspects are also briefly presented. In this context, two approaches are considered: (i) overview of the current available technologies for the abatement of NOx, with special focus being on the selective catalytic reduction process (SCR); (ii) theoretical view upon the deNOx process by mathematical modeling in order to describe the phenomena occurring in the deNOx reactor.

1.1. Introduction: the NOx Problem

Nitrogen shows several types of oxides due to the multitude of oxidation states this element possesses. These nitrogen oxides are: N_2O (nitrous oxide), NO (nitric oxide), NO_2 (nitrogen dioxide), N_2O_3 (dinitrogen trioxide), N_2O_4 (dinitrogen tetroxide), and N_2O_5 (dinitrogen pentoxide). Among these nitrogen oxides, NO, NO_2 and N_2O are of utmost importance, due to their harmful environmental impact. These three nitrogen oxides are also called "fresh" nitrogen oxides, since they reach the atmosphere in these forms [2]. The abbreviation NOx, mostly encountered in the scientific literature, designates the gaseous mixture formed by NO and NO_2 [2–4].

1.1.2. Sources of NOx

Nitrogen oxides are formed in gas–phase reactions, during combustion processes at high temperatures [5–7]. In an internal combustion engine, where high temperatures occur, N and O combine with each other yielding nitrogen oxides: under stoichiometric conditions nitric oxide (NO) is predominant, while under lean conditions (excess oxygen), nitric oxide is oxidized to nitrogen dioxide (NO_2) [7]. It is generally agreed upon the classification of the NOx formation routes: *thermal* NOx, *fuel* NOx, and *prompt* NOx [3,6–8]. NOx are also formed by natural causes such as oxidation of ammonia, lightning or volcano activities, but their prevalence is limited, and the associated negative environmental impact is minor [2]. NOx sources may be classified not only by the formation mechanism of these pollutants, but also by the emitting entity. Such a classification is illustrated in Fig. 1.1 using the data provided in [4]. Authors generally agree upon this classification, and tend to simplify it by delimiting two category sources: (1) mobile sources with a share of approximately 54 %, and (2) stationary sources with a share around 46 % [9].

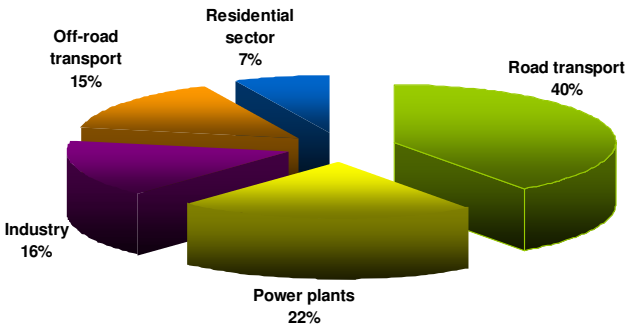

Fig. 1.1. Estimation of the anthropogenic NOx sources: the represented data were taken from [4]**.**

1.1.3. Environmental impact of NOx emissions

Among the constituent NOx components, NO_2 is more toxic than NO. High or consistent exposures to NO_2 cause respiratory and cardiovascular problems, and even death, in extreme cases [2]. NO, the major component of NOx, causes irritation of soft tissues (e.g. eye, throat) [2,15]. Numerous other environmental problems are caused by the emissions of NOx into the atmosphere: acid rain, photochemical smog, greenhouse effects, fine particles in the atmosphere, etc [2,7,16,17].

1.2. Abatement of NOx emissions

The large variety of NOx sources and the consequent diversity of NOx containing exhaust gases, lead to the development of different control technologies, appropriate and dedicated to each particular case. Among these different control technologies two main strategies can be distinguished: (1) the *combustion modification strategy* (also called *primary control*), applied before or during the combustion process, or (2) the *exhaust after treatment strategy* (also called *secondary control*), which is applied for the reduction of NOx content in the resulted flue gases [6,28]. In particular cases, a combination between these two approaches may also be adopted.

1.2.2. Secondary control technologies

Exhaust after–treatment techniques, as the term suggests, involve the treatment of exhaust gases resulted in combustion processes or special chemical plants, in order to reduce harmful emissions in general, and NOx in particular. Two trends may be distinguished in this case: (i) either *removal* of NOx by physical processes (adsorption on activated carbon, or absorption in alkaline solutions), or (ii) *destruction* of NOx by their transformation to benign products through chemical or biochemical processes [2]. After–treatment involving the transformation of NOx into harmless products is generally achieved by chemical processes

such as: (1) *reduction* (catalytic or non–catalytic selective reduction – SCR or SNCR, respectively); (2) *oxidation* (non–thermal plasma oxidation – NTP [30], use of O_3 as oxidant [31], or photocatalytic oxidation – PCO [32,33]); (3) *decomposition of NOx* (requires a high activation energy [16,34]); (4) *electron beam method* (process based on the interaction of NOx with radiation [35,36]). Combinations between these methods may also be applied [31,37,38]. The chemical methods based on the reduction process of NOx using different reducing agents are most widely spread, for both mobile and stationary sources [34].

1.2.2.1. Selective Non–Catalytic Reduction (SNCR)

The *non–catalytic* selective reduction approach consists in the reaction of NOx present in the exhaust gases with a particular reducing agent, at temperatures between 850–1175°C [8]. The advantages of SNCR are: (i) simple technical approach as no catalysts is needed (several catalysts' problems can be avoided); (ii) easy retrofitting in existing stationary facilities; (iii) reduced investment and operating costs [8,39]. The most important drawbacks of the SNCR technology are: (i) the relatively narrow and high temperature window; (ii) lower deNOx efficiency; (iii) easier slip of reducing agent (NH_3) [5,39].

1.2.2.2. Selective Catalytic Reduction (SCR)

The *catalytic* selective reduction of NOx requires a catalyst to lower the activation energy needed for the reduction of NOx by a certain reducing agent. It is a heterogeneous process, the reactions occurring in the gas–solid system. This approach is not a new one, the first SCR systems being used for stationary sources at the end of the 1970s in Japan, while in Europe this technology was first used in 1985 [15]. A high versatility can be attributed to this technology, due to its possible application for both mobile and stationary sources. The most important advantages of the SCR technology are: (i) high deNOx efficiencies, up to 90 %; (ii) applicability to emitters with low NOx concentrations (ppm level); (iii) lower reaction temperatures required, leading to energy savings; (iv) modifications of the emitting source are not required [42]. Several drawbacks should also be mentioned: (i) higher capital and operating costs due to catalyst use; (ii) fouling or deactivation of catalyst may occur due to the presence of other components in the flue gases; (iii) cleaning of downstream equipment might be needed [42].

According to Savva and Costa four possible ways for the selective catalytic reduction of NOx can be distinguished [43]:

(1) NH_3–SCR involves the reduction of NO by ammonia, in the presence of O_2:

$$4NO + 4NH_3 + O_2 \rightarrow 4N_2 + 6H_2O \quad (1.1)$$

$$NO + NO_2 + 2NH_3 \rightarrow 2N_2 + 3H_2O \quad (1.2)$$

$$6NO_2 + 8NH_3 \rightarrow 7N_2 + 12H_2O \quad (1.3)$$

Several problems may arise in the application of this process, although up to now it is the best available current technology (BACT): ammonia slip, ammonia transport and storage, ash odor, or fouling (plugging of air heaters) [2,43].

(2) CO–SCR is mostly encountered in three–way–catalysis (TWC), a technology used for mobile sources, which enables the concomitant elimination of three combustion pollutants: NOx, CO and hydrocarbons (HC). In this approach, the used catalyst facilitates the oxidation of CO and HC, and the reduction of NOx simultaneously [28]. Reduction of NO by CO occurs according to the following reaction [7]:

$$2NO + 2CO \rightarrow N_2 + 2CO_2 \quad (1.6)$$

(3) HC–SCR is based on the idea of reusing the unburned or partially combusted hydrocarbons from the fuel, in order to reduce the NOx resulted from the combustion process [16,43,46]. The reduction process may be described by the general reaction [16]:

$$4NO + C_xH_y + (4x + y - 4)/4\ O_2 \rightarrow 4N_2 + xCO_2 + y/2\ H_2O \quad (1.7)$$

but the chemistry involved is much more complex.

(4) H_2–SCR has attracted attention only in the last two decades, as it was long believed that H_2, as well as CO could not be efficient in the reduction of NOx. Armor recognized the potential use of hydrogen as reducing agent, but considered it a too valuable chemical feedstock [16]. However, development of hydrogen production technologies from renewable sources, besides the classical technologies, brought H_2 into a new light.

1.3. Selective Catalytic Reduction with Hydrogen (H_2–SCR)

1.3.1. Hydrogen – an efficient reducing agent for NOx

The growing interest in "green chemistry" based technologies led to an increased focus on hydrogen. Reduction of NO by H_2 is described by the reactions (1.8) – (1.10), resulting in the formation of N_2, N_2O, and NH_3 as N reduced species [61]:

$$2NO + 2H_2 \rightarrow N_2 + 2H_2O \quad (1.8)$$

$$2NO + H_2 \rightarrow N_2O + H_2O \quad (1.9)$$

$$2NO + 5H_2 \rightarrow 2NH_3 + 2H_2O \quad (1.10)$$

In the presence of O_2, however, NO is reduced according to the following reactions [59]:

$$2NO + 4H_2 + O_2 \rightarrow N_2 + 4H_2O \quad (1.11)$$

$$2NO + 3H_2 + O_2 \rightarrow N_2O + 3H_2O \quad (1.12)$$

$$2H_2 + O_2 \rightarrow 2H_2O \quad (1.13)$$

One of the most important advantages in using H_2 as reducing agent for NO is given by the fact that reduction occurs by a clean, environmental friendly agent. By this approach, use of a harmful chemical compound to abate another pollutant is avoided. On the other hand, compared to NH_3–SCR, the costs involved with the reducing agent are decreased because H_2 is an intermediate in the NH_3 production technology. Thus, use of H_2 instead of ammonia is straightforward. Nonetheless, it should not be disregarded that "clean" H_2–SCR is debatable if H_2 used is produced form fossil fuels. In such a case, H_2 is an indirect source of CO_2 [43,60]. Another important advantage of H_2–SCR is that it allows energetic costs minimization due to the possibility of lowering the necessary reduction temperature. Several authors reported efficient deNOx by hydrogen at reduction temperatures below 150–200°C, depending on the catalysts used [62,63].

1.3.2. Catalysts used for H_2–SCR

A large variety of catalysts were already reported to be efficient in the H_2–SCR process. However, most of these catalysts are noble metals based, and only a few are of other type. Noble metals and semi–precious metals are the best choice for H_2–SCR catalysts because these metals do not allow the inhibition effect of oxygen for the NO + H_2 reaction as it occurs in case of other catalysts [43]. The noble metals of choice, generally Pt, Pd, Rh, Ir, are supported on different oxides or zeolites. In our opinion, the most important contributions in the development of H_2–SCR catalysts were brought by the groups of Efstathiou at the University of Cyprus in Nicosia, and Granger from the University of Science and Technology in Lille (France), respectively. Efstathiou et al. dedicated in developing catalytic materials with low noble metal content which could be efficient in the catalytic reduction of NOx by H_2, under operation conditions similar to those occurring in stationary sources (e.g. power plants for which exhaust gases contain important amounts of SO_2, PM, O_2, etc). Thus, they developed a new catalyst, Pt (0.1wt.%)/CeO_2–MgO, which could be successfully applied for industrial applications [59,62,65]. Mechanistic studies were also performed with the aim of elucidating the support influence upon the reduction of NO by H_2 in strongly oxidizing conditions [66–68]. The group of Granger, on the other hand, focused on kinetic studies for different catalysts, both in the absence and presence of oxygen

in the reaction mixture. Special focus was dedicated to the Pd based catalysts, either supported on γ–Al_2O_3 [63,69,70], or on a new supporting material, $LaCoO_3$ [69,71,72].

1.4. Reactor types for NOx abatement

Depending on the deNOx technology of choice, a large variety of reactors can be used for the abatement of nitrogen oxides. For example, in case of selective non–catalytic reduction (SNRC), solutions of ammonia or urea are injected into the radiant or convection zone of a coal fired boiler where they reduce NOx in a high, but narrow temperature range, usually 870–980°C [6]. Considering, however, that most of the secondary NOx control strategies are based on the selective catalytic reduction approach, the vast majority of deNOx reactors are of catalytic type. Moreover, selection and/or design of catalytic reactors for the deNOx process of choice is dependent on a series of factors, such as catalyst type, properties of the reactants, residence time, reaction temperature, pressure, mass and heat transfer phenomena, etc [73]. In a recent review by Cheng and Bi (2014), SCR reactors for stationary applications were classified into three categories: (1) structured reactors; (2) fluidized bed reactors; and (3) moving bed reactors [74].

1.5. Mathematical modeling of the catalytic deNOx reactor

1.5.1. Why mathematical modeling?

Three main purposes for pursuing mathematical modeling of a process can be considered: (1) *description* of the performance or behavior of the process; (2) *justification /explanation* of the occurrence of specific behaviors or results in the system; or (3) *prediction* of outputs in case of other modifications in the system, which cannot be foreseen or obtained by experimental methods. The third purpose is of utmost importance in engineering sciences in general, and in chemical engineering in particular, because it allows cost savings due to the fact that expensive and time consuming experiments can be spared. However, the experimental part should not be disregarded, mostly because each mathematical process model must be validated by experimental results. Thus, a good interconnectivity between experimental techniques and mathematical modeling can lead to better performances of the process considered.

1.5.2. Mathematical models for SCR reactors

There has been a growing interest in developing mathematical models for the catalytic deNOx reactors in the last decades [88], dedicated to a quite large range of

applications. However, the majority of them are dedicated to NH_3–SCR reactors with monolith catalysts in the form of honeycomb, due to the larger spreading of this technology in industry. One of the first models was proposed by Tronconi et al. [89] and consisted in a one–dimensional (1D) reactor model based on a rate equation of Eley–Rideal type. Several other mathematical models were proposed since then by their group, also with kinetic and reactor model adaptations for catalytic converters for mobile sources [90,91]. Schaub et al. proposed an isothermal pseudo–homogeneous model for a catalytic filter in which reduction of NO occurs also via NH_3 [92]. It should be highlighted here that most of these models are one–dimensional ones, 2D or 3D models being proposed only later on by Dhanushkodi et al. [3] and Chen & Tan [93], respectively. Fewer models were proposed by now for SCR systems using other reducing agents than ammonia. Thus, for CO–SCR a one–dimensional axially dispersed plug flow reactor model was proposed by Makeev and Peskov [94], while for ethanol–SCR Kim et al. proposed a comprehensive kinetic model together with simulation results of the steady state reactor model [95]. In case of H_2–SCR, the group of Balakotaiah developed several reactor models, either in the absence [96] or in the presence of oxygen [97]. In both cases, the model accounts for a honeycomb monolith reactor. Attempts to describe by mathematical modeling bi–functional reactors were also provided, for example in case of a NSR–SCR converter Zuckerman et al. proposed a 1D model accounting for the mass and heat balances in both units [88]. Moreover, additionally to an analytical 1D model, Faghihi and Shamekhi developed an artificial neural network based model which allows much faster run–times [98].

CHAPTER 2
Catalyst preparation and experimental methods

This chapter describes the preparation methods of both mono– and bimetallic alumina supported catalysts, as well as the experimental techniques used for their physico–chemical characterization (BET surface area and pore characteristics, XRD, TPR, H_2–TPD, NO–TPD). All experimental methods employed for the investigation of the catalytic performance are depicted, with detailed description of the used experimental set–up. The algorithms used for the evaluation of the catalytic activity parameters are also presented.

2.1. Catalyst preparation

A large variety of preparation methods can be considered for the synthesis of heterogeneous catalysts: precipitation or co–precipitation method, deposition–precipitation, sol–gel techniques, impregnation or co–impregnation, hydrothermal method, etc [99–101].

The supported noble metal catalysts were obtained by the wet impregnation method on alumina prepared in the laboratory by the precipitation method, according to the procedures presented in two of our published papers [102,103]. Alumina support thus prepared was impregnated with the appropriate aqueous solutions of $H_2PtCl_6 \cdot 6H_2O$ (Alfa Aesar, 99.9 %), $Pd(NO_3)_2 \cdot xH_2O$ (Alfa Aesar, 99.9 %), or $RhCl_3 \cdot xH_2O$ (Sigma–Aldrich, 99.9 %) in order to obtain catalysts with noble metal loadings of 1 wt.%. After impregnation, the catalysts were dried at room temperature for 24 h, calcined at 450°C under continuous Ar flow for 4 h, and finally reduced at 450°C under H_2 flow for another 4 h.

Ni based catalysts, unpromoted or promoted by low amounts of noble metals, were obtained by the impregnation method for Ni/Al_2O_3 or by co–impregnation method for the bimetallic catalysts, using commercially available alumina (Alfa Aesar, S_{BET} =134 m^2/g) (also see our published papers [61,104]). The Ni/Al_2O_3 (10 wt.% Ni) catalyst was obtained by impregnation of the alumina support with the appropriate amount of $Ni(NO_3)_2$ aqueous solution ($Ni(NO_3)_2 \cdot 6H_2O$, 98 % from Alfa Aesar). In case of bimetallic catalysts, mixed solutions with the appropriate amounts of the metal precursors of interest were used in order to obtain metal loadings of 10 wt.% for Ni and 0.5 wt.% for the promoting noble metal. The impregnated/ co–impregnated catalysts were dried at room temperature overnight, then 2 h at 100°C in an oven, followed by calcination at 550°C for 3 h under continuous Ar flow, and finally the reduction step at 550°C for 3 h under continuous H_2 flow.

The catalysts obtained from metal chloride precursors were repeatedly washed with distilled water in order to remove the remaining Cl^- ions.

2.2. Characterization techniques

2.2.1. BET total surface area and pore characteristics

Determination of total surface area relies upon the physical adsorption of a gas onto the surface of a porous material and uses the Brunauer–Emmett–Teller (BET) method. N_2 *adsorption – desorption isotherms* were measured by means of a Sorptomatic 1990 apparatus (Thermo Electron, USA) at –196°C. Prior to the adsorption measurements, each sample was degassed under vacuum at 200°C, for 3 hours. Specific surface areas of the samples were estimated from the adsorption isotherm data in the relative equilibrium pressure interval of 0.02–0.3 p/p_0. Specific pore volume was evaluated using the Dollimore–Heal method, which relies on the Kelvin equation and on the cylindrical pore model [106]. Mean pore radii were estimated using the desorption branch in the 0.01–0.95 p/p_0 range.

2.2.2. X–ray powder diffraction (XRD)

X–ray diffraction is a very versatile and widely used method for the characterization of the bulk crystalline structure and for the estimation of the average crystallite dimensions. However, very small particles (< 3–5 nm) cannot be detected by XRD, and only an average crystallite dimension can be estimated, without any information about the particle size distribution. X–ray diffractograms were recorded on a Bruker D8 Advanced Diffractometer with Cu Kα1 radiation and a Ge monochromator, working at 40 kV and 40 mA. A step scanning mode of $\Delta 2\theta$ = 0.01°/s was used in the angle range 2θ = 15–85°. The average crystallite size was estimated by means of Scherrer's equation [107].

2.3. Temperature programmed characterization techniques

Temperature programmed reaction techniques are widely used for the characterization of catalytic materials as these methods provide important information, are relatively cheap and do not require sophisticated equipments. These techniques consist in monitoring the development of a reaction while increasing the T with a certain rate.

2.3.1. Temperature programmed reduction (TPR)

The TPR technique is widely used for the investigation of metal supported catalysts, as it gives information about the metallic species present after impregnation and the strength of their interaction with the support. It also indicates the necessary temperature for the complete reduction of the catalyst [107]. TPR performed for bimetallic catalysts can indicate if the two metallic species are in contact or not, and how well they are mixed on the support.

For the TPR analyses a Microactivity Reference Reactor (PID Eng & Tech, Spain) with a stainless steel tubular reactor of 9 mm i.d. coupled to a mass spectrometer (PrismaPlus, Pfeiffer Vacuum, Germany) was used. A sample mass of ~0.5 g from the calcined catalyst was placed inside the reactor while *T* was increased by 10°C/min from ambient temperature to 750°C, under 50 mL/min flow of the reducing mixture consisting in H_2 in Ar (10 vol.%). Consumption of H_2 was continuously monitored by MS [61,104].

2.3.2. H_2–temperature programmed desorption (H_2–TPD) and metal dispersion

TPD analysis provides useful information about the type and strength of active catalytic centers for the chemisorption of different species (H_2, NH_3, NO, CO, etc). Such experiments can give an insight into the reaction mechanism of a certain catalytic process. For the specific case of the NO reduction by hydrogen, temperature programmed desorption of H_2 (H_2–TPD) and NO (NO–TPD) were performed in order to investigate the chemical interaction of the reaction species with the catalytic surface involved.

H_2–TPD analyses for the noble metal supported catalysts were performed by means of the Microactivity Reference Reactor – Mass Spectrometer coupling. A catalyst sample mass of ~2 g was used in each run. Adsorption of hydrogen was performed at room temperature (25°C) or at 150°C for 30 min using a mixture of H_2 in Ar (5 vol.% in case of the Pd (2wt.%)/Al_2O_3 catalyst, and 20 vol.% for the noble metal catalysts with 1 wt.% loadings). After H_2 chemisorption at 150°C the catalyst sample was cooled to room temperature under H_2 flow, and then cleaned under Ar for 30 min in order to remove the physisorbed hydrogen species in the catalyst bed. Temperature was ramped by 5°C/min in case of Pd (2wt.%)/Al_2O_3, or by 20°C/min in case of the other noble metal catalysts. Prior to any H_2–TPD experiment, catalysts were activated in situ under H_2 flow at 300°C for 30 min.

In case of the Ni based catalysts a TPDRO 1100 Series equipment (Thermo Scientific) was used. Experiments consisted in the increase of *T* from ambient to 1100°C, by a rate of 10°C/min, under 20 mL/min Ar flow. Prior to H_2–TPD spectrum recording by means of a TCD, each sample (~0.35 g) was pretreated as follows: reduction, under H_2 flow (20 mL/min, 10.1 vol.% H_2 in Ar) at 550°C for 3 h, cooling down to 50°C, followed by surface cleaning under 20 mL/min Ar flow for 1 h, surface saturation at 50°C with H_2 (20 mL/min, 10.1 vol.% H_2 in Ar) for 1 h, and, finally, cleaning with Ar (20 mL/min) for 30 min, at 50°C [61,104]. Metal dispersion (percent of exposed metal atoms in the catalyst) was evaluated using the amount of desorbed H_2. A stoichiometry of one hydrogen atom per

surface metal atom was considered, that is $M/H_2 = 2$. In case of bimetallic catalysts it was assumed that the surface metal concentrations were equal to the bulk concentration.

2.3.3. NO–temperature programmed desorption (NO–TPD)

Except otherwise stated, adsorption of NO was done at 150°C by passing NO (0.5 vol.% in Ar) with 25 mL/min flow, for 0.5 h over each catalyst sample of 0.5 g. The catalyst was then cooled to room temperature under 25 mL/min (NO + Ar) flow, and then purged under Ar flow for 0.5 h in order to remove the weakly adsorbed NO molecules. Temperature was then increased by a ramp of 10°C/min up to 750°C and desorption products were continuously analyzed by MS. Prior to any NO–TPD experiment, the samples were activated in H_2 at 350°C, for 1 h, and then cleaned and cooled to 150°C under Ar flow [61,102].

2.4. Catalytic activity tests

2.4.1. Experimental set–up

Catalytic activity investigations were carried out in the Microactivity Reference Reactor (PID Eng & Tech, Spain) coupled to the quadrupole mass spectrometer (PrismaPlus, Pfeiffer Vacuum, Germany) by means of a capillary, which can be heated up to 200°C in order to avoid condensation of gases. The reactor consists in a stainless steel tube (i.d. 8 or 9 mm) which can be heated up to 800°C by means of an electric furnace (Fig. 2.2).

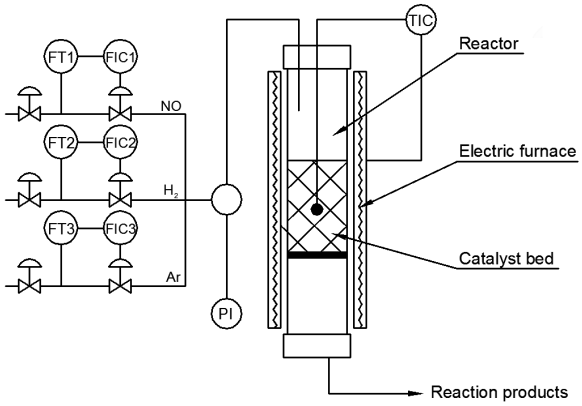

Fig. 2.2. Experimental set–up used for the catalytic activity studies.

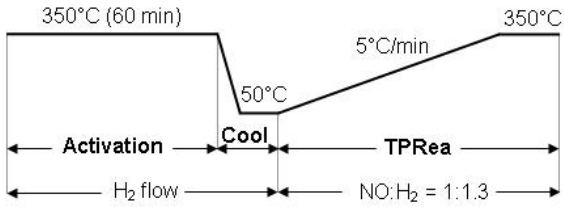

Fig. 2.3. Experimental sequences in the temperature programmed reaction runs.

All catalytic activity tests were carried out at atmospheric pressure. Generally, catalyst sample masses of ~1 g were loaded in the tubular reactor. Feeds with different NO concentrations in Ar were employed (1.8 %, 1 % or 0.5 % v/v NO in Ar). Preliminary catalytic studies consisted in exploring the influence of several parameters on the catalyst's activity, such as: reaction temperature (T), NO concentration in the feed ($[NO]^{in}$), molar ratio between reactants (NO/H_2), or gas hourly space velocity ($GHSV$). Prior to any catalytic

test, catalyst samples were reduced in situ for 1 h, under H_2 flow at 350°C. After the reduction step, the catalyst and all lines were cleaned with Ar and cooled to the reaction temperature of interest. The outlet gas composition was analyzed by means of the coupled MS by monitoring the following mass numbers (*m/z*): 2 for H_2, 15 for NH_3, 28 for N_2, 30 for NO, 32 for O_2, 44 for N_2O, and 46 for NO_2.

2.4.2. Temperature programmed NO + H_2 reactions (TPRea)

In the case of temperature programmed NO + H_2 reactions (TPRea) the catalyst samples were loaded reactor and heated up to 350°C with a rate of 5°C/min (schematics in Fig. 2.3). A total feed rate of 75 mL/min was used, which corresponds to a *GHSV* of 4500 h^{-1}. The feed consisted of 0.5 % NO, 0.65 % H_2, and Ar as balance gas, corresponding to a reactant molar ratio NO/H_2 of 1:1.3. Plug flow conditions were ensured by complying to the criteria due to Froment et al. [109]. Effluent gases were monitored by MS, as detailed above.

2.4.3. Stability tests

Stability tests consisted in the investigation of the time on stream (TOS) on the activity of the catalysts under study. This means that the reaction was monitored at the selected reaction conditions (*T*, NO/H_2, *GHSV*) for a specific time range (*t*) in order to evaluate the deactivation probabilities and the catalytic performance in time.

2.4.4. Data evaluation

Conversion (*X*) of a reactant at temperature *T* is defined as the amount of reactant transformed into products divided by the amount of the same reactant in the reaction feed. In case of NO, the degree of conversion is given by:

$$X_{NO} = \frac{[NO]^{in} - [NO]^{out}}{[NO]^{in}} \times 100,\ (\%) \qquad (2.5)$$

Selectivity (*S*) for a certain reaction product is defined as the amount of that product formed due to the transformation of reactants. Selectivity for N_2 was evaluated according to:

$$S_{N_2} = \frac{2[N_2]^{out}}{[NO]^{in} - [NO]^{out}} \times 100,\ (\%) \qquad (2.6)$$

Yield (*Y*) of a certain product is a parameter which cumulates the catalyst's activity for NO reduction with its performance towards the formation of this product, N_2 in our case.

$$Y_{N_2} = X_{NO} \cdot S_{N_2},\ (\%) \qquad (2.7)$$

CHAPTER 3
Alumina supported noble metal catalysts for the reduction of NO by hydrogen

Pd (2wt.%)/Al_2O_3 was used as probe catalyst for the determination of optimal reaction conditions in the reduction of NO by H_2. Several parameters were varied in order to evaluate their influence over the catalytic performance: reaction temperature (T), reactants molar ratio (NO/H_2), NO concentration in the feed ($[NO]^{in}$), or gas hourly space velocity (GHSV). Catalytic activity results showed that the most important influence is given by the reaction temperature and GHSV. Lower loadings of noble metals on the alumina support were also envisaged for the reduction of NO by H_2. Thus, Pt (1wt.%)/Al_2O_3, Pd (1wt.%)/Al_2O_3 and Rh (1wt.%)/Al_2O_3 catalysts were comparatively tested in this reaction using the previously established best reaction conditions. The most efficient catalyst proved to be the Pd one, with NO conversion values of at least 90 % and N_2 selectivity of 85 % already at 75–100°C. The catalytic performance increases in the series: Rh (1wt.%)/Al_2O_3 < Pt (1wt.%)/Al_2O_3 < Pd (1wt.%)/Al_2O_3. The results discussed in this chapter were presented in two of our previously published papers [102,103].

3.1. Introduction

Noble metal based catalysts have been considered for the catalytic reduction of NO resulted from both stationary [15,65] and mobile sources [2,10]. In case of stationary sources, use of noble metal based catalysts was abandoned due to their ability to oxidize NH_3 during the process [15]. It should be reminded here that, currently, the BACT for the reduction of NOx resulted from stationary sources is the ammonia based one (NH_3–SCR), with its main drawback the slip of NH_3 into the atmosphere.

Along with the possibility of using H_2 as reducing agent for the abatement of NOx, noble metal catalysts have regained research interest due to their ability to chemisorb both involved reactants: NO and H_2. Lately, H_2 has been envisaged as reducing agent for NOx resulted from stationary sources as well. Hence, catalysts developed for stationary applications use the model three way catalysts (TWC) as start point, but have generally high noble metal loadings, i.e. up to 3 wt.%. Several noble metal based catalysts have been developed for industrial applications such as Pt catalysts (Pt/MgO–CeO_2 [65], Pt/La_2O_3, Pt/SiO_2, Pt/CaO [59], Pt/TiO_2 [59,111], Pt/Ti–MCM–41 [112]), or some Pd catalysts (Pd/SiO_2, Pd/MgO, Pd/Al_2O_3 with 2 wt.% Pd [113]) which have been proved to be active for NOx reduction at temperatures below 300°C.

The aim of this chapter is to provide an insight into the specifics of the reduction of NO by hydrogen as reducing agent over alumina supported noble metal catalysts. Thus, Pd

(2wt.%)/Al_2O_3 catalyst prepared by impregnation of 'home–made' alumina was first investigated in order to establish the best experimental reaction conditions. Second, noble metals (Pt, Pd and Rh) deposited on alumina in lower loadings (1 wt.%) were comparatively tested in the same reaction, using the established reaction conditions.

3.3. Pd (2wt.%)/Al_2O_3 – probe catalyst for the determination of optimal reaction conditions

3.3.1. Catalyst characterization (BET, XRD)

Impregnation of the precipitated Al_2O_3 in order to obtain a Pd loading of 2 wt.% leads to a decrease of both specific surface area and pore characteristics. BET surface area decreases from 232.5 m^2/g in case of γ–Al_2O_3, to 190.8 m^2/g for the Pd/Al_2O_3 catalyst. Pores of the Pd catalyst are narrower, with mean pore radii of 1.75 nm compared to 1.92 nm for the support, while the specific pore volume is 0.18 cm^3/g compared to 0.26 cm^3/g for Al_2O_3. Both Al_2O_3 and Pd catalyst are mesoporous materials as proven by the type IV adsorption–desorption isotherm and have a narrow pore size distribution (Fig. 3.1). The very broad diffraction lines corresponding to γ–Al_2O_3 at 37.2°, 45.6° and 66.9° prove the precipitated alumina as an amorphous material. In case of Pd (2wt.%)/Al_2O_3, Pd is present only in the metallic form (Fig. 3.2) with crystallite sizes evaluated around 540 Å.

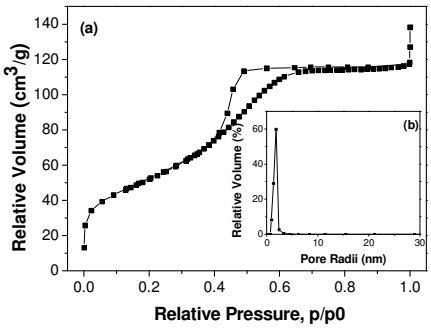

Fig. 3.1. (a) N_2 adsorption–desorption isotherms and (b) pore size distribution for Pd (2wt.%)/Al_2O_3 (support prepared by precipitation).

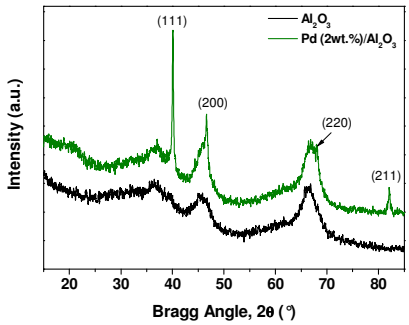

Fig. 3.2. XRD patterns for the prepared alumina support and for Pd (2wt.%)/Al_2O_3 (marked lines correspond to Pd diffraction planes).

3.3.2. Catalytic activity tests

3.3.2.1. Temperature influence

In order to have some preliminary information on the influence of the reaction temperature over the catalytic performance of Pd (2wt.%)/Al_2O_3, temperature programmed NO + H_2 reaction was performed in the range of 50 to 350°C, using a rate of 5°C/min. Among the possible reaction products, only N_2, N_2O and H_2O were detected under these

reaction conditions. Formation of neither NO_2 nor NH_3 was observed. Conversion of NO rapidly increases at T up to 100°C. At this temperature, NO is converted up to 71 %, while at 110°C, NO conversion exceeds 95 %. No significant change in the conversion of NO can be noticed at T > 110°C. The conversion profile of the reducing agent presents a less accentuated increase with temperature, H_2 conversions higher than 85 % being reached at T > 200°C. The influence of T over the formation of products is more significant (Fig. 3.4). Thus, formation of N_2O is enhanced at T < 150°C, with a maximum at 110°C. However, at T > 175°C, N_2O is practically absent in favor to the formation of N_2, the desired reaction product. Our results are consistent with the observations reported for other catalysts as well, e.g. Pt (5wt.%)/SiO_2 [118], Rh (0.2wt.%)/Al_2O_3 [119], PdMOR or CePdMOR [117], etc.

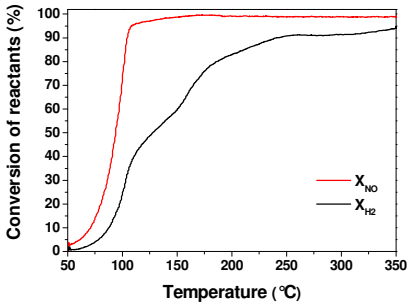

Fig. 3.3. NO and H_2 conversion on Pd (2wt.%)/Al_2O_3 as a function of temperature (NO/H_2 = 1:1.1, $GHSV$ = 6,000 h^{-1}, $[NO]^{in}$ = 1.8 %).

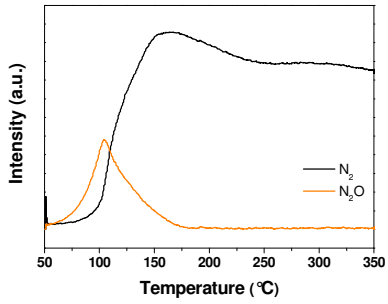

Fig. 3.4. Temperature influence on the formation of products on Pd (2wt.%)/Al_2O_3 (NO/H_2 = 1:1.1, $GHSV$ = 6,000 h^{-1}, $[NO]^{in}$ = 1.8 %).

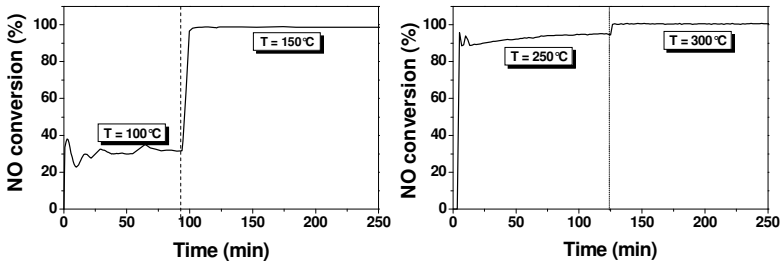

Fig. 3.6. Conversion profiles of NO on Pd (2wt.%)/Al_2O_3 in temperature step reactions (reaction conditions: NO/H_2 = 1:1.25, $GHSV$ = 12,000 h^{-1}, $[NO]^{in}$ = 1.0 %).

The influence of the reaction temperature on the reduction of NO by H_2 was also investigated by performing stability tests at five different temperatures (Fig. 3.6). Except for the profile at 100°C, in all other cases steady state is reached shortly after the switch to the next reaction temperature. Already at 150°C, NO is almost totally converted to reaction products, X_{NO} exceeding 98 % at each T value.

Both temperature programmed reaction experiments and stability tests performed at different working temperatures lead to the conclusion that reduction of NO by hydrogen can be performed already at 150°C with NO conversion values greater than 98 % and N_2 selectivities above 70 %.

3.3.2.2. Effect of reactants molar ratio (NO/H_2)

Several ratios were selected around stoichiometry as presented in Fig. 3.7 and 3.8. The obtained NO conversion values show that reactants ratio close to unity are adequate for the achievement of maximum conversion. Use of excess H_2 does not lead to superior conversion values. Reactants ratios below unity lead to slightly lower conversion values (Fig. 3.7), and higher selectivities towards the formation of N_2O (Fig. 3.8). No significant differences concerning S_{N2O} arise by varying the reactants ratio close or above unity at the selected working temperature (150°C). These results reveal a slight increase of NO conversion compared to the results presented in the previous section at the same working temperature, due to the lower *GHSV*.

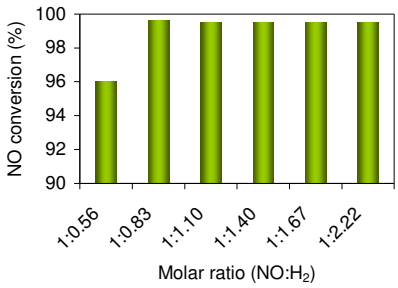

Fig. 3.7. Conversion of NO on Pd (2wt.%)/Al_2O_3 as a function of reactants molar ratio (T = 150°C, $GHSV$ = 6,000 h^{-1}, $[NO]^{in}$ = 1.8 %).

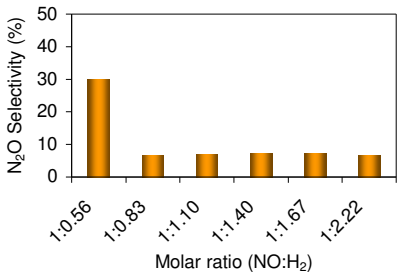

Fig. 3.8. Formation of N_2O (S_{N2O}) on Pd (2wt.%)/Al_2O_3 as a function of reactants molar ratio (T = 150°C, $GHSV$ = 6,000 h^{-1}, $[NO]^{in}$ = 1.8 %).

3.3.2.3. Effect of NO concentration in the feed

During the investigation for best reaction conditions in case of Pd (2wt.%)/Al_2O_3, two mixtures of NO in Ar were employed: 1 vol.% and 1.8 vol.%. These concentrations of NO in the gaseous feed mixture were thus selected as to correspond to the concentration range of the exhaust gases resulted in the operation of the ^{15}N separation column. NO conversion values shown in Fig. 3.10 (a) and (c) prove that the concentration of NO in the feed does not significantly influence the degree of NO conversion. Thus, at 100°C conversion values around 30 % are obtained for both concentrations, while at 150°C NO conversion reaches 98 %. Distribution of reaction products, as well, is not significantly

different due to the variation of NO concentration in the feed. N_2O selectivity is higher at 150°C compared to 100°C, in accordance to the observation that a maximum of N_2O formation is reached at *T* between 110–160°C (see also Fig. 3.4).

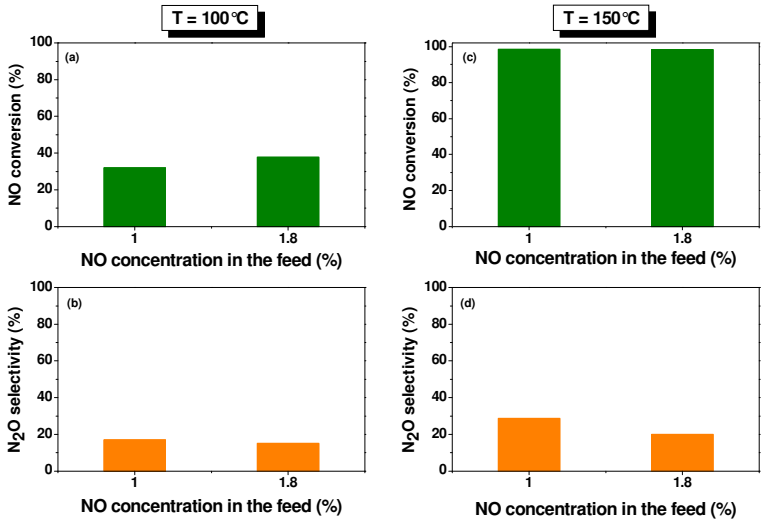

Fig. 3.10. Effect of NO concentration in the reactants feed over the degree of NO conversion and the selectivity towards N_2O on Pd (2wt.%)/Al_2O_3, at two temperatures (*GHSV* = 12,000 h^{-1}, NO/H_2 = 1:1.25).

3.3.2.4. Effect of gas hourly space velocity (GHSV)

Gas hourly space velocity (GHSV) relates the reactants gas flow rate to the reactor volume or catalyst volume and it is calculated by [120, pp. 530]:

$$GHSV = \frac{\text{Volumetric flow rate of the feed at STP } (m^3/h)}{\text{Reactor or catalyst volume } (m^3)} \ (h^{-1}) \qquad (3.1)$$

It may be observed that one way of varying the values of the *GHSV* is to vary the volumetric flow rate of the feed, while maintaining the volume of the catalyst sample used. In our specific case, a catalyst sample mass of 1 g, with a bulk volume of ~1 g/cm^3, was diluted with 1 g of quartz with the same bulk density. *GHSV* values were calculated by dividing the various volumetric flow rates used by the volume of the catalyst sample. Thus, three values of the *GHSV* were experimentally investigated: 3,000, 6,000 and 12,000 h^{-1}, respectively. The catalytic activity results show that this parameter influences mostly the distribution of the reaction products, and not so much the degree of NO conversion. It may be observed that by increasing the *GHSV*, the conversion of NO decreases slightly, from 99 % at 3,000 h^{-1} to 98 % at 12,000 h^{-1} (Fig. 3.11). N_2O selectivity, on the other hand, increases with increasing *GHSV*, reaching 20 % at 12,000 h^{-1} (Fig. 3.12). This means that formation of N_2 in the reduction of NO by H_2 is favored by lower *GHSV* values.

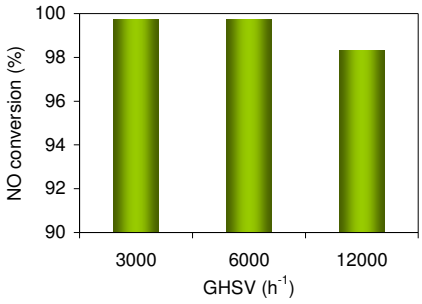

Fig. 3.11. Effect of *GHSV* on the conversion of NO (reaction conditions: Pd (2wt.%)/Al_2O_3, T = 150°C, NO/H_2 = 1:1.25, $[NO]^{in}$ = 1.8 %).

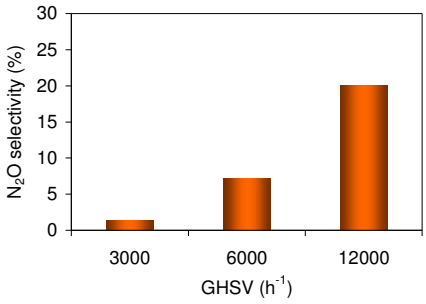

Fig. 3.12. Effect of *GHSV* on the formation of N_2O (reaction conditions: Pd (2wt.%)/Al_2O_3, T = 150°C, NO/H_2 = 1:1.25, $[NO]^{in}$ = 1.8 %).

3.4. Alumina supported noble metal catalysts with 1 wt.% loading for the reduction of NO by H_2: A comparative study

This Section presents the catalytic activity performance of noble metal supported alumina catalysts, with metal loadings of 1 wt.%, at reaction temperatures below 350°C. Catalysts reported in the literature with low noble metal loadings are generally intended for vehicular exhaust applications, and not for the removal of NOx resulted from stationary sources. Catalysts proposed for comparative investigation are Pt (1wt.%)/Al_2O_3, Pd (1wt.%)/Al_2O_3, and Rh (1wt.%)/Al_2O_3. These catalysts were tested under the reaction conditions established in Section 3.3 in case of Pd (2wt.%)/Al_2O_3.

3.4.1. Physico–chemical characterization of catalysts (BET, XRD)

N_2 adsorption–desorption isotherms reveal that all supported noble metal catalysts, as well as alumina alone, present a type IV isotherm, characteristic to mesoporous materials. Impregnation of the precipitated alumina support with noble metals leads to a decrease of both BET specific surface area and pore characteristics (Table 3.2).

Table 3.2. Specific surface area (S_{BET}), pore specific volume (V_p), and average pore radius (R_m) of the support and noble metal catalysts.

Catalyst	S_{BET} (m^2/g cat)	V_p (cm^3/g)	R_m (nm)
Al_2O_3	245	0.22	1.74
Pt/Al_2O_3	209.3	0.17	1.69
Pd/Al_2O_3	220.6	0.19	1.73
Rh/Al_2O_3	210.6	0.18	1.70

XRD measurements did not evidence diffraction lines corresponding to either of the noble metals. This could be explained by the low metal loadings, but also by the fact that the deposited metal particles are quite small (not shown here).

3.4.2. Temperature programmed desorption of reactants

3.4.2.1. H_2–temperature programmed desorption (H_2–TPD)

H_2–TPD profiles have a similar shape, desorption peaks being centered to similar temperatures; desorption amplitudes, however, are distinct suggesting a different behavior towards the adsorption of hydrogen, from the quantitatively point of view. Thus, it may be observed that the amount of desorbed hydrogen decreases in the following series order: Pt (1wt.%)/Al_2O_3 > Pd (1wt.%)/Al_2O_3 ≥ Rh (1wt.%)/Al_2O_3 > Al_2O_3 (Fig. 3.17).

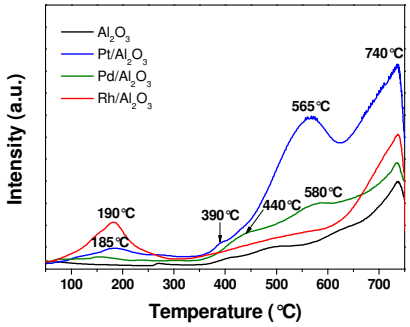

Fig. 3.17. Hydrogen desorption profiles for Al_2O_3, Pt (1wt.%)/Al_2O_3, Pd (1wt.%)/Al_2O_3, and Rh (1wt.%)/Al_2O_3 (H_2 chemisorption at 150°C, temperature rate of 20°C/min).

3.4.2.2. NO–temperature programmed desorption (NO–TPD)

NO temperature programmed desorption experiments were carried out on the support alone, as well as on the noble metal supported alumina in order to get a hint about the types of catalytic active centers and to investigate the adsorption behavior of the reactant, NO, as well as the desorption behavior of the resulted N species. Fig. 3.18 shows that chemisorption of NO at 150°C on each sample is followed by desorption of NO, N_2, and N_2O. Desorption of neither NO_2 nor NH_3 was evidenced in our experimental conditions. The presence of these desorption species indicates that NO adsorption on the catalytic surface occurs molecularly, as well as dissociatively, dissociated NO being further converted to N_2 and N_2O (consistent with the desorption behavior observed for Pd (2wt.%)/Al_2O_3). NO–TPD profiles suggest that the presence of noble metals (Pt, Pd, Rh) on the alumina surface enhances the adsorption of NO, as well as its dissociation to form N_2 or N_2O. Desorption peaks of NO centered at

temperatures below 200°C confirm the finding of Granger et al. that at low temperatures (< 150°C) noble metal sites are essentially covered by strongly NO species [130].

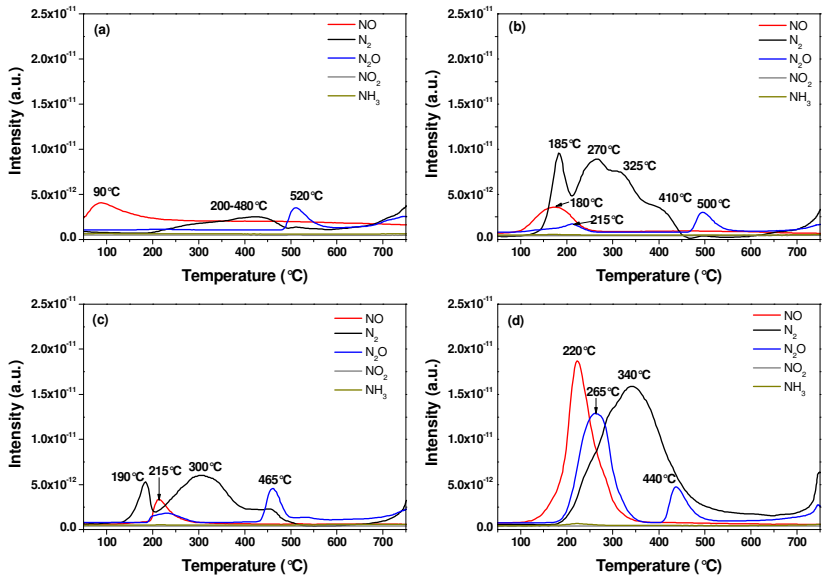

Fig. 3.18. TPD profiles of NO, N_2, N_2O, NO_2 and NH_3 obtained after adsorption of NO at 150°C on (a) Al_2O_3, (b) Pt (1wt.%)/Al_2O_3, (c) Pd (1wt.%)/Al_2O_3, and (d) Rh (1wt.%)/Al_2O_3 (temperature rate of 20°C/min).

3.4.3. Catalytic activity measurements

3.4.3.1. Temperature programmed reaction (TPRea)

In case of the noble metal supported alumina catalysts with 1 wt.% metal loading, TPRea runs evidenced that NO is reduced by hydrogen to form N_2 and H_2O as main reaction products, while N_2O is formed as byproduct. The presence of neither NO_2 nor NH_3 was evidenced in the effluent gases.

NO conversion increases with rising temperature in case of each catalyst (Fig. 3.19). For the Pt and Pd catalysts, X_{NO} shows a similar behavior with increasing *T*. At 50°C, X_{NO} for Pt is more than double than for Pd (40 %, compared to 16 %, respectively), but it increases more rapidly for the latter one, so that both catalysts exhibit similar X_{NO} values at 75°C (92 % for Pt, and 94 % for Pd). In the *T* range of 75–200°C, the Pd catalyst shows superior X_{NO} values than Pt, the largest gap occurring at 150°C. The Rh catalyst shows a very different behavior, so that X_{NO} increases more slowly with increasing *T*, reaching only ~27 % up to 150°C, but increases very rapidly up to 200°C, where it achieves 96 %. At *T* > 200°C all noble metal catalysts exhibit $X_{NO} > 95$ %.

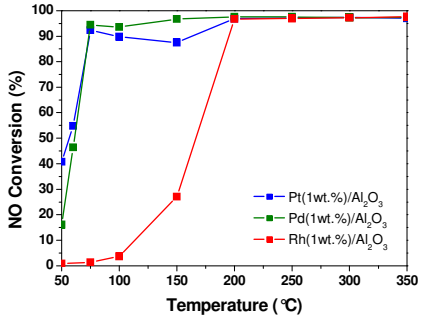

Fig. 3.19. X_{NO} in the temperature programmed NO + H_2 reaction on Pt (1wt.%)/Al_2O_3, Pd (1wt.%)/Al_2O_3 and Rh (1wt.%)/Al_2O_3 (T = 50–350°C, 5°C/min, $GHSV$ = 4,500 h^{-1}, NO/H_2 = 1:1.2, $[NO]^{in}$ = 0.5 %).

Table 3.3. Temperatures for $X_{NO} = 50$ % and $X_{NO} = 90$ %.

Catalyst	T_{50} (°C)	T_{90} (°C)
Pt (1wt.%)/Al_2O_3	59	68
Pd (1wt.%)/Al_2O_3	61	68
Rh (1wt.%)/Al_2O_3	162	181

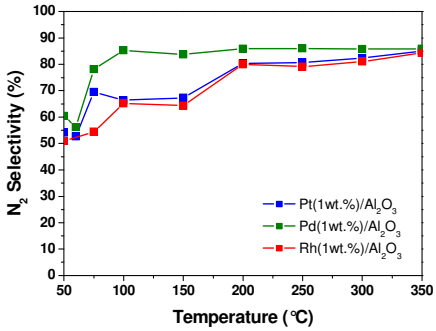

Fig. 3.20. N_2 selectivity (S_{N2}) in the TP NO + H_2 reaction on Pt (1wt.%)/Al_2O_3, Pd (1wt.%)/Al_2O_3 and Rh (1wt.%)/Al_2O_3 (50–350°C, 5°C/min, $GHSV$ = 4,500 h^{-1}, NO/H_2 = 1:1.2, $[NO]^{in}$ = 0.5 %).

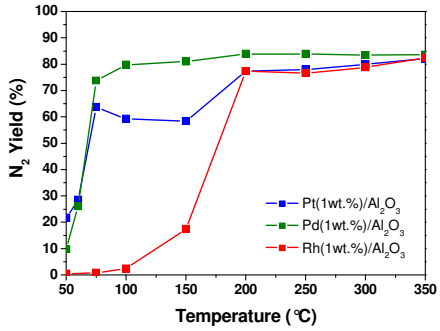

Fig. 3.21. N_2 yield (Y_{N2}) in the TP NO + H_2 reaction on Pt (1wt.%)/Al_2O_3, Pd (1wt.%)/Al_2O_3 and Rh (1wt.%)/Al_2O_3 (50–350°C, 5°C/min, $GHSV$ = 4,500 h^{-1}, NO/H_2 = 1:1.2, $[NO]^{in}$ = 0.5 %).

Performance of catalysts was also evaluated by assessing the temperature needed for half NO conversion (T_{50} for X_{NO} = 50 %), or the temperature for a conversion of 90 % (T_{90}). Both T_{50} and T_{90} reinforce the conclusion that in respect to X_{NO} at low temperatures, Pt and Pd catalysts are very similar, and both are significantly superior to the Rh one (Table 3.3).

In terms of N_2 selectivity, the Pd catalyst appears to be the most promising one (Fig. 3.20). Hence, S_{N2} values for this catalyst are superior to those corresponding to either Pt or Rh, over the whole investigated temperature range (50–350°C). Already at 75°C it reaches 80 %, compared to 70 % for Pt and 54 % for Rh, respectively. Starting with reaction

temperatures above 100°C, S_{N2} for Pd (1wt.%)/Al_2O_3 shows values around 85 %. Except for the 50–100°C temperature range, both Pt and Rh catalyst exhibit similar S_{N2} values, approaching 85 % only at 300°C.

Evaluation of N_2 yield better highlights the superiority of the Pd catalyst in contrast to the other two investigated ones (Fig. 3.21). It may be observed that starting with 75°C, Y_{N2} for Pd (1wt.%)/Al_2O_3 is at least 75 %, exceeding 80 % at each reaction temperature above 100°C. Neither Pt nor Rh catalysts approach these values at any reaction temperature, except for 300°C where all three catalysts present similar Y_{N2} values. The slightest increase with reaction temperature occurs in case of the Rh catalyst.

TPRea experiments have shown that there is a strong influence of the temperature upon the catalytic activity of all three investigated noble metal catalysts. The most active catalyst is Pd (1wt.%)/Al_2O_3 considering NO conversion, as well as N_2 selectivity or N_2 yield. It may be concluded that catalytic performance in the reduction of NO by H_2 increases in the following series order: Rh (1wt.%)/Al_2O_3 < Pt (1wt.%)/Al_2O_3 < Pd (1wt.%)/Al_2O_3.

3.4.3.2. Stability tests

The effect of time on stream (TOS) over the performance of catalysts was studied for several reaction temperatures in case of each sample. Stability tests thus performed are presented here only for Pd (1wt.%)/Al_2O_3, the most active catalyst in the reduction of NO by H_2.

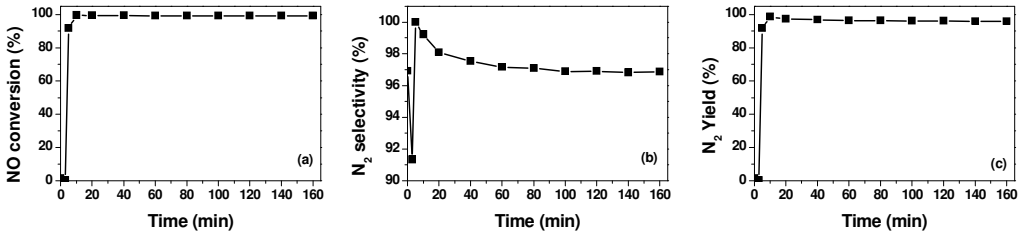

Fig. 3.22. Effect of TOS on the conversion of NO (a), N_2 selectivity (b) and N_2 yield (c) in case of the Pd (1wt.%)/Al_2O_3 catalyst (reaction conditions: T = 150°C, $GHSV$ = 9,000 h^{-1}, NO/H_2 = 1:1.5, $[NO]^{in}$ = 0.5 %).

In case of the Pd catalyst, if X_{NO} or Y_{N2} are considered, it may be observed that steady state is reached readily, in only 10 min of reaction (Fig. 3.22 (a) and (c)). The steady state values are ~99 % for X_{NO}, and ~96 % for Y_{N2}. Steady state for N_2 selectivity is reached after a longer time on stream (~60 min), when ~96–97 % is attained (Fig. 3.22 (b)). This behavior

in case of S_{N2} is consistent with the observed MS profiles of the effluent gases obtained during the reaction on Pd (2wt.%)/Al_2O_3 (Fig. 3.5).

3.5. Conclusions

Alumina supported noble metal catalysts prove to be efficient in the reduction of NO by H_2 at T < 350°C. The reaction products for each catalyst are N_2, H_2O and N_2O as byproduct. Formation of neither NO_2 nor NH_3 was observed under these reaction conditions.

The best reaction conditions were investigated for Pd (2wt.%)/Al_2O_3. It was shown that among the various investigated parameters (T, NO/H_2, *GHSV*, $[NO]^{in}$) the reaction temperature has the greatest effect upon the catalytic performance. A stoichiometry close to unity suffices for almost total reduction of NO by H_2, as well as for attaining the best N_2 selectivity. NO concentration in the feed has no significant influence upon either of the catalytic parameters. *GHSV* mostly influences the selectivity in N_2, and not the conversion of NO. Thus, better N_2 selectivities, and also N_2 yields are favored by lower *GHSV*s.

In the investigated series of noble metal catalysts with lower metal loadings (1wt.%), the Pd one proved to be the most efficient. Already at temperatures around 75–100°C, NO conversion values are above 90 %, while selectivity in N_2 is at least 85 %. In respect to NO conversion the catalytic performance of the Pt catalyst is close to that corresponding to Pd, but N_2 selectivities and N_2 yields are inferior. The Rh catalyst is the most inefficient one, good catalytic activity being attained only at T > 200°C. Chemisorption of either reactants (NO or H_2) is enhanced by the presence of the noble metals on the alumina support, while H_2 assists the dissociation of NO to form either of the reduced species (N_2 or N_2O).

CHAPTER 4

Alumina–supported nickel based catalysts for the reduction of NO by H_2: Promotion by Pt, Pd and Rh

Use of the common Ni/Al_2O_3 catalyst was envisaged for the reduction of NO by hydrogen due to its lower costs. The promotional effect of low concentrations of noble metals (Pt, Pd and Rh) on the alumina supported Ni catalyst was also considered. Thus, $Ni(10wt.\%)/Al_2O_3$ and the promoted homologues with 0.5 wt.% loadings of noble metals ($Ni–Pt/Al_2O_3$, $Ni–Pd/Al_2O_3$, and $Ni–Rh/Al_2O_3$) were tested in the reduction of NO by H_2.
Characterization techniques revealed that promotion with small amounts of noble metals enhances the reducibility of the supported NiO in the catalyst precursor, as well as the dispersion of the metal on the catalyst surface. Catalytic activity tests consisting in temperature programmed reactions (TPRea) and stability tests at different temperatures, under plug flow conditions reveal that the most efficient catalyst in the NO + H_2 reaction is $Ni–Pd/Al_2O_3$, with NO conversions greater than 95 % and N_2 selectivity of at least 90 % at $T \geq 100°C$. Unexpectedly, although both Ni and Rh are efficient in the dissociative adsorption of NO (as shown by NO–TPD experiments), the catalytic performance of the $Ni–Rh/Al_2O_3$ catalyst proved to be only slightly superior to that corresponding to Ni/Al_2O_3.
The results reported in this chapter were presented in two of our published papers [61,104].

4.1. Introduction

The main set–back for the replacement of the current best available SCR technology (NH_3–SCR) for stationary sources with a hydrogen based one, is the high cost of the necessary catalysts. H_2–SCR catalysts are mostly based on noble metals with loadings up to 3 wt.% deposited on different supports [102,111,133]. In order to minimize the costs of the catalysts in the overall technology, lower loadings of noble metals should be used, without compromising the catalytic performances. For this purpose, two approaches can be considered: (1) use of reducible materials as support, due to the involvement of both metal and support sites in the reaction mechanism [130,134]; or (2) promotion of lower cost base metals with noble metals [135]. Supported bimetallic catalysts have drawn considerable attention lately due to the possibility of one constituent metal to improve or to modify the catalytic properties of the other metal [136,137]. Several bimetallic catalysts were reported by now for H_2–SCR in stationary sources: $Pd(0.63wt.\%)–Co(0.58wt.\%)/Al_2O_3$ [138], $Pt(1.3wt.\%)–Ni(0.0265wt.\%)/Al_2O_3$ [139], $Pt(1.3wt.\%)–Co(0.0265wt.\%)/Al_2O_3$ [140], $Pd(0.9wt.\%)–Ir(Rh)(0.9wt.\%)/TiO_2$ [133]. Results presented in this chapter are aimed to prove the beneficial effect of low amounts of noble metals used as promoters for the common and cheap Ni/Al_2O_3 (10 wt.% Ni) catalyst in the NO reduction by H_2.

4.3. Results and discussions

4.3.1. Textural properties of catalysts

4.3.1.1. BET surface area and pore characteristics

Impregnation of the alumina support with either Ni alone or Ni promoted with Pt, Pd or Rh leads to a decrease of both total surface area (S_{BET}) and pore characteristics (V_p , R_m) (Table 4.1). Promoted Ni catalysts present similar surface areas as compared to the unpromoted one. Regarding the pore specific volume, all catalysts show similar values, except for the Ni–Rh catalyst which exhibits a slightly increased value. According to the IUPAC classification [105], the alumina support as well as the prepared Ni based catalysts present a type IV adsorption–desorption isotherm, characteristic to mesoporous adsorbent materials, and have a very narrow pore size distribution.

Table 4.1. Textural properties of the catalysts.

Catalyst	S_{BET} (m^2/g cat)	V_p (cm^3/g)	R_m (nm)	d_{Ni}^{XRD} (nm)	d_{NM}^{XRD} (nm)	D_M (%)
Al_2O_3	134	0.256	2.61	–	–	–
Ni/Al_2O_3	105.2	0.176	2.73	12.27	–	4.57
Ni–Pt/Al_2O_3	107.3	0.178	2.75	4.37	–	10.43
Ni–Pd/Al_2O_3	104.0	0.174	2.76	6.45	15.75	6.86
Ni–Rh/Al_2O_3	107.2	0.191	2.78	4.75	–	7.42

S_{BET} – Specific surface area; V_p – pore specific volume; R_m – average pore radius (nm); d_{Ni}^{XRD} – Ni crystallite size; d_{NM}^{XRD} – noble metal (NM) crystallite size; D_M – metal dispersion.

4.3.1.2. XRD results

Each catalyst samples shows characteristic peaks assigned to γ–Al_2O_3 (37.3°, 45.7° and 67.1°) and to metallic Ni (44.5° for Ni(1 1 1), 51.8° for Ni(2 0 0) and 76.5° for Ni(2 2 0)) (figure not shown here). However, in case of the noble metal promoted catalysts, Ni diffraction lines are slightly broadened and lowered in amplitude. On the other hand, the recorded diffraction patterns prove that nickel is present in each catalyst sample only in the metallic form, due to the absence of diffraction lines corresponding to other Ni species such as NiO or $NiAl_2O_4$. Except for the Ni–Pd catalyst, diffraction lines corresponding to the promoting noble metals could not be distinguished in the recorded XRD patterns. This is most probably due to the low concentration of noble metal loadings. Results presented in Table 4.1 show that Ni crystallites size are significantly decreased in the case of bimetallic catalysts due to the promotional effect of Pt, Pd and Rh.

4.3.2. Temperature programmed surface reactions

4.3.2.1. Temperature programmed reduction (TPR) results

Temperature programmed reduction (TPR) was used in order to investigate the influence of the promotional noble metals on the reducibility of Ni^{2+} ions in the alumina supported nickel catalysts, which can be further used to evaluate the strength of the Ni–support interaction [146]. The unpromoted Ni/Al_2O_3 catalyst presents a large reduction peak at 730°C and a shoulder around 500°C. It is debatable whether the high temperature peak is given by $NiAl_2O_4$ [146] or by NiO strongly interacting with the alumina support [147], so much more as XRD patterns previously discussed do not show any evidence of either of these Ni species. The reduction peak situated at lower temperature may be attributed to NiO in weaker interaction with the support [145]. The reduction profiles of the noble metal promoted catalysts differ significantly from the Ni/Al_2O_3 corresponding one, due to the change of the ratio between the amplitude of the peaks assigned to the two types of NiO interacting with the support. TPR experiments prove that promotion with low amounts of noble metals strongly influences the reducibility of NiO. Several literature reports stated that this enhancement of the Ni reducibility due to the presence of noble metals suggests a close proximity of the metals in the bimetallic catalyst structure [128,147].

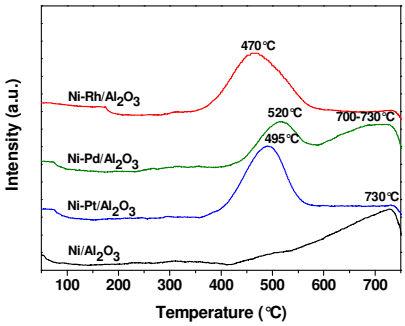

Fig. 4.3. TPR profiles of Ni/Al_2O_3, Ni–Pt/Al_2O_3, Ni–Pd/Al_2O_3, and Ni–Rh/Al_2O_3 (5°C/min).

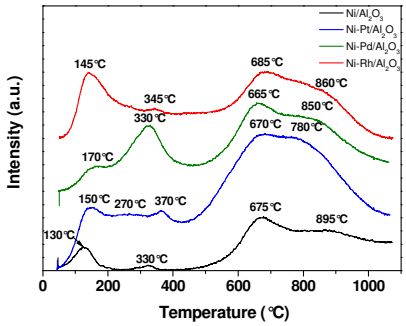

Fig. 4.4. H_2–TPD profiles for Ni/Al_2O_3, Ni–Pt/Al_2O_3, Ni–Pd/Al_2O_3, and Ni–Rh/Al_2O_3 (H_2 chemisorption at 50°C, desorption under Ar flow,10°C/min).

4.3.2.2. H_2–temperature programmed desorption (H_2–TPD) and metal dispersion

Temperature programmed desorption of H_2 was used to investigate the type and strength of active catalytic centers for hydrogen chemisorption and activation. H_2–TPD profiles point out that H_2 desorption occurs at different temperatures (Fig. 4.4). Depending on the strength of the previously formed hydrogen–superficial metal bonds, four desorption peaks may be distinguished in case of all investigated catalysts. These desorption peaks are

situated at similar temperatures, but with different amplitudes, proving thus that all catalysts present catalytic centers of similar type. A closer evaluation of the H_2–TPD spectra reveals the separation of two desorption regions: (i) one region situated at lower temperatures (< 500°C), and (ii) the second region corresponding to higher temperatures (> 500°C). Other literature reports denoted these domains as type–1 and type–2 desorption peaks, respectively [150,151]. Type–1 peaks are attributed to hydrogen desorbed from Ni nanoparticles, while type–2 peaks are considered to correspond to hydrogen deposited on subsurface layers and/or spiltover hydrogen. Hydrogen desorption profiles in case of all three noble metal promoted Ni catalysts present larger peaks, proving that hydrogen chemisorption occurs on these catalytic surfaces to a larger extent than on the monometallic one. The H_2 desorption profile in case of Ni–Pd/Al_2O_3 stands out in the series, mostly due to the fact that the ratio between the peaks in the type–1 region is reversed.

Quantitative assessment of H_2–TPD spectra reveals that promotion with either of the considered noble metals enhances the total metal dispersion, namely the H_2 chemisorption capacity of the catalysts (91.82 μmol H_2/g_{cat} for Ni–Pt/Al_2O_3, 59.91 μmol H_2/g_{cat} for Ni–Pd/Al_2O_3, and 64.90 μmol H_2/g_{cat} for Ni–Rh/Al_2O_3, compared to 38.86 μmol H_2/g_{cat} for Ni/Al_2O_3). Metal dispersion increases in the following series order: Ni/Al_2O_3 < Ni–Pd/Al_2O_3 < Ni–Rh/Al_2O_3 < Ni–Pt/Al_2O_3 (Table 4.1). This enhancement of the metallic dispersion may be explained by the presence of Pt, Pd or Rh on the catalytic surface, which leads to an increasing number of active metal sites [147,152].

4.3.2.3. NO–temperature programmed desorption

Nickel is expected to be active in the adsorption of NO, but the influence of the promoting noble metals upon the extent and type of NO adsorption may only be evaluated by proper surface investigations. Thus, NO–TPD runs were carried out on Ni/Al_2O_3, as well as on the noble metal promoted catalysts, in order to investigate the chemical interaction of NO with the catalytic surface. In case of the Ni based catalysts, adsorption of NO was done only at 150°C, and not at room temperature, as well, (as for Pd(2wt.%)/Al_2O_3). Choice of this adsorption temperature was due to the fact that promising catalytic activity was observed starting with this value of the reaction temperature. NO–TPD spectra obtained after NO adsorption at 150°C showed that three nitrogen containing molecules are desorbed from the catalytic surface: NO, N_2, and N_2O (Fig. 4.5), proving that adsorption of NO on the catalytic surface occurs both molecularly and dissociatively. TPD spectra obtained for Ni/Al_2O_3 show that both molecular and dissociative species coexist on Ni/Al_2O_3, the ratio being shifted

towards the latter ones (Fig. 4.5 (a)). On the other hand, it may be observed that these two adsorption paths for NO may be associated with two temperature domains: (i) the low temperature region assigned to molecularly adsorbed NO (T < 300°C), and (ii) the high temperature region assigned to dissociatively adsorbed NO (T > 300°C). Promotion by noble metals seems to enhance the NO adsorption capacity of the bimetallic catalysts, especially for Ni–Pt and Ni–Rh catalysts, either for the molecular or the dissociative path.

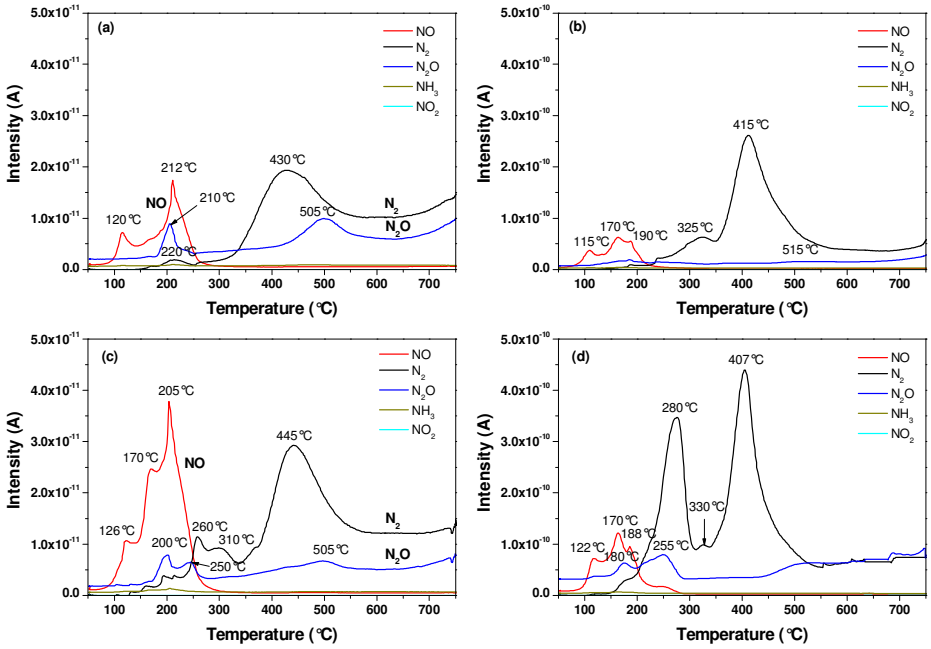

Fig. 4.5. TPD profiles of NO, N_2, N_2O obtained over (a) Ni/Al_2O_3; (b) $Ni–Pt/Al_2O_3$; (c) $Ni–Pd/Al_2O_3$; (d) $Ni–Rh/Al_2O_3$; NO adsorption at 150°C, desorption under Ar flow, temperature rate of 10°C/min.

4.3.3. Catalytic activity measurements

4.3.3.1. Temperature programmed reaction (TPRea)

In case of the Ni based catalysts as well, the only reaction products to be detected by the MS are N_2, N_2O and H_2O. Formation of neither NH_3 nor NO_2 was observed under these reaction conditions, so that for Ni catalysts as well, only reactions (1.8) and (1.9) are considered. TPRea in the 50–350°C temperature range reveal that conversion of NO increases with increasing reaction temperature for Ni/Al_2O_3, as well as for the promoted Ni catalysts, reaching similar values at reaction temperatures above 200°C. However, in the lower temperature range, i.e. T < 200°C, promotion by Pt, Pd or Rh leads to an improvement of the NO conversion extent. In the promoted catalyst series, $Ni–Pd/Al_2O_3$ shows the best conversion values: already at 100°C, NO conversion exceeds 95 %, while at temperatures

above 150°C, X_{NO} is greater than 98 %. Ni–Pt/Al_2O_3, on the other hand, gives NO conversion values above 80 % only at T > 130°C, but reaches 98 % at 150°C, as well as the Pd promoted catalyst. In case of Ni–Rh/Al_2O_3, inferior conversion values are obtained compared to the other two promoted catalysts, 80 % being reached only at 140°C.

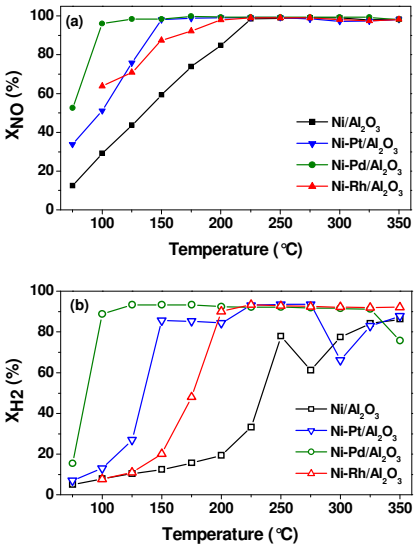

Fig. 4.6. (a) NO conversion (X_{NO}) and (b) H_2 conversion (X_{H2}) in the TP NO + H_2 reaction on Ni/Al_2O_3, Ni–Pt/Al_2O_3, Ni–Pd/Al_2O_3 and Ni–Rh/Al_2O_3 (50–350°C, 5°C/min, $GHSV$ = 4,500 h^{-1}).

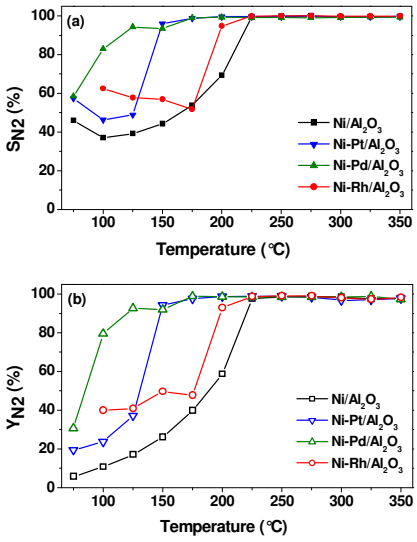

Fig. 4.7. (a) N_2 selectivity (S_{N_2}) and (b) N_2 yield (Y_{N_2}) in the TP NO + H_2 reaction on Ni/Al_2O_3, Ni–Pt/Al_2O_3, Ni–Pd/Al_2O_3 and Ni–Rh/Al_2O_3 (50–350°C, 5°C/min, $GHSV$ = 4,500 h^{-1}).

Table 4.2. Temperatures for the attainment of 75 % and 95 % NO conversion.

Temperature/Catalyst	Ni/Al_2O_3	Ni–Pt/Al_2O_3	Ni–Pd/Al_2O_3	Ni–Rh/Al_2O_3
T_{75} [°C] (for X_{NO} = 75 %)	178	125	87	132
T_{95} [°C] (for X_{NO} = 95 %)	218	145	98	186

Table 4.2 presents the temperatures at which 75 % or 95 % conversion of NO is reached in case of each catalyst. It may be observed that for each conversion target, the Pd promoted catalyst exhibits the best catalytic performance, followed at an appreciable distance by the Pt and Rh promoted ones. In respect to NO conversion, the catalytic performance of the investigated catalysts increases in the series order Ni–Pd/Al_2O_3 > Ni–Pt/Al_2O_3 > Ni–Rh/Al_2O_3 > Ni/Al_2O_3 at reaction temperatures below 225°C. However, at higher reaction temperatures their catalytic performance is quite similar under these reaction conditions.

Hydrogen conversion does not increase as fast as NO conversion during the (NO + H_2) reaction, despite the reactants ratio close to stoichiometry (Fig. 4.6 (b)). Thus, H_2 conversion approaches 90 % only at 350°C, in case of the unpromoted Ni catalyst. H_2

conversion values in case of the promoted catalysts show that the presence of noble metals in the Ni/Al_2O_3 catalyst is beneficial, however the difference between these bimetallic catalysts seems augmented compared to the degree of NO conversion.

A high degree of reactants conversion is important only if the chemical transformation leads to the formation of reaction products with minimum content of by–products. Thus, N_2 selectivity in case of Ni/Al_2O_3 increases slowly with increasing reaction temperature, reaching 70 % at 200°C, while at temperatures above 200°C, the slope changes, so that S_{N_2} of 95 % is achieved at 220°C (Fig. 4.7 (a)). Ni–Rh/Al_2O_3 exhibits only slightly better N_2 selectivities compared to the monometallic catalyst. The Pt promoted catalyst presents only slightly improved values at temperatures below 125°C, but at T > 150°C, N_2 selectivity approaches the values obtained in case of Ni–Pd/Al_2O_3. The Pd promoted catalyst exhibits the best N_2 selectivity values over the entire temperature range. Thus, S_{N_2} values as high as 95 % are obtained at 125°C, and 98 % at 175°C.

In respect to N_2 yield, all promoted catalysts show superior values than the unpromoted Ni catalyst alone (Fig. 4.7 (b)). However, Ni–Rh/Al_2O_3 shows only slightly superior N_2 yield values, compared to Ni/Al_2O_3 in the 150–350°C temperature range. In contrast, promotion by Pd yields N_2 productions of 80 % already at 100°C, while N_2 yields greater than 90 % are achieved at T > 125°C. Ni–Pt/Al_2O_3 shows the same behavior in respect to N_2 yield as the Ni–Pd catalysts, only at temperatures above 150°C.

It was expected that both Ni and Rh, known for their ability to easily dissociate NO and to recombine the resulted N atoms to form N_2, would show the best catalytic performance in the NO reduction process. TPD experiments of both reactants (H_2–TPD and NO–TPD) performed for Ni–Rh/Al_2O_3 evidenced that activation of either NO or H_2 occurs easily on this catalytic surface, in contrast however with the relatively low catalytic performance compared to the other two promoted Ni catalysts. Two reasons could be accounted for this peculiar behavior of the Ni–Rh catalyst: (i) either the reduction of NO by hydrogen occurs preferentially via molecularly adsorbed NO, or (ii) the extensive dissociative adsorption of NO occurring on the Ni–Rh catalyst inhibits the dissociation of H_2 molecules. Based on our characterization results and other literature reports, it was concluded that enhanced dissociative adsorption of NO on either Ni/Al_2O_3 or its promoted equivalent, Ni–Rh/Al_2O_3, does not lead to better catalytic performances of these catalysts in the NO + H_2 reaction, primarily due to the involved reaction mechanism in which molecularly adsorbed NO react with chemisorbed H atoms.

The catalytic performance of the Pd promoted Ni catalyst is also surprising. The extent of molecular adsorption of NO occurring on the catalytic surface is the most plausible explanation. However, the formation of palladium hydrides, PdH_x, during the reduction sequence of the catalyst prior to catalytic activity tests [63,128] should not be excluded. These palladium hydrides could provide additional amounts of hydrogen, which can be further available for the reduction of NO. This hypothesis might be supported also by the different H_2–TPD profile obtained for Ni–Pd/Al_2O_3, compared to the other three catalysts, especially in the lower temperature range (Fig. 4.4). The outlines of NO reduction on the Pd promoted catalyst are schematically illustrated in Fig. 4.8 [61].

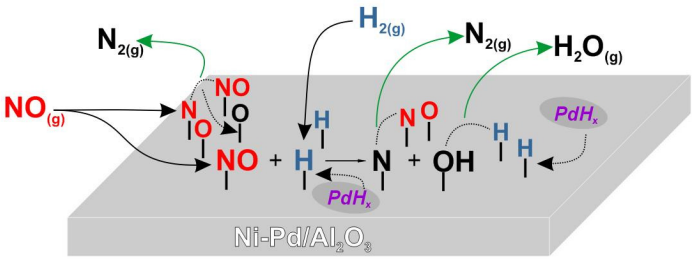

Fig. 4.8. Schematic representation of NO + H_2 reaction on Ni–Pd/Al_2O_3 [our work 61].

4.3.3.2. Effect of time on stream on X_{NO} (%) and S_{N2} (%)

Efficient catalysts for a specific reaction require not only good catalytic performance values (conversion, selectivity), but also good stability under prolonged and heavy reactants exposure. Hence, stability tests reveal that stable catalytic activity parameters are obtained after approximately two hours time on stream in case of each catalyst (Fig. 4.9). In spite of this relatively rapid stability settlement, catalytic activity parameters are considerably lower than those obtained during the TPRea tests, especially for Ni/Al_2O_3 and Ni–Rh/Al_2O_3. Ni–Pd/Al_2O_3 is the only catalyst from the investigated series that holds similar catalytic activity performances during the stability tests as those obtained from the TPRea experiments. Hence, at 100°C, X_{NO} stabilizes around 97 % (very close to 95 % from TPRea), while S_{N_2} approaches 85 % (Fig. 4.9 (e)). On the other hand, at 250°C, NO is practically totally converted, with corresponding N_2 selectivity around 98 % (Fig. 4.9 (f)).

It may be concluded that stability tests, as well, prove the Pd promoted Ni catalyst as the most efficient one in the studied catalyst series, so much more as very good performances are achieved already at 100°C, meeting thus all established performance criteria.

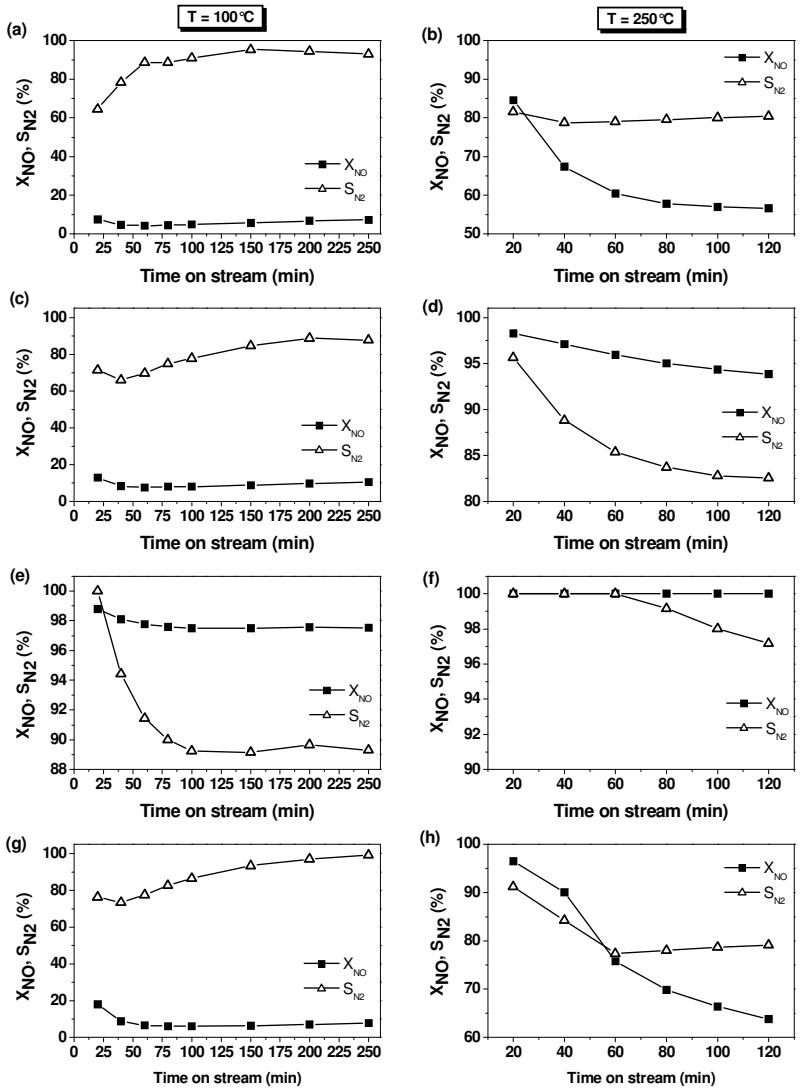

Fig. 4.9. Effect of time on stream on X_{NO} (%) and S_{N_2} (%) at T = 100°C and T = 250°C for (a)–(b) Ni/Al_2O_3; (c)–(d) Ni–Pt/Al_2O_3, (e)–(f) Ni–Pd/Al_2O_3, (g)–(h) Ni–Rh/Al_2O_3 (NO/H_2=1:1.3, *GHSV* = 4,500 h^{-1}).

4.3.3.3. Cost analysis of the noble metal promoted catalysts

Catalytic activity results presented and discussed above prove that promotion of Ni/Al_2O_3 by small amounts of Pd might be an interesting alternative towards the costs minimization in the H_2–SCR process. This goal may be achieved due to (i) the possibility of reaction temperature decrease which leads to lower energetic costs, and (ii) the decrease of the catalyst cost. The economical advantage of the noble metal promoted Ni based catalysts over catalysts with higher noble metal loadings (*e.g.* 1 wt.%) may be evidenced by a catalyst cost estimation, considering only the price of raw materials. The estimated costs reveal that

each bimetallic catalyst is almost two times cheaper than the corresponding noble metal based one. This rough estimation shows that catalyst costs may be reduced by 50 % if noble metals are replaced by cheap base metals (e.g. Ni), but still promoted with very low amounts of precious metals in order to preserve similar catalytic performances in the process.

Table 4.3. Estimated catalysts' cost considering only the price of the constituent components.

Catalyst	Cost ($/kg)
Pt (1%)/Al_2O_3	540
Ni (10%)–Pt (0.5%)/Al_2O_3	278
Pd (1%)/Al_2O_3	272
Ni (10%)–Pd (0.5%)/Al_2O_3	144
Rh (1%)/Al_2O_3	392
Ni (10%)–Rh (0.5%)/Al_2O_3	203

4.4. Conclusions

Ni(10wt.%)/Al_2O_3, as well as its noble metals promoted equivalents: Ni(10wt.%)–Pt(0.5wt.%)/Al_2O_3, Ni(10wt.%)–Pd(0.5wt.%)/Al_2O_3, and Ni(10wt.%)–Rh(0.5wt.%)/Al_2O_3 were comparatively tested in the reduction of NO by hydrogen, at reaction temperatures below 350°C. Characterization techniques (XRD, TPR, H_2–TPD) proved that promotion by Pt, Pd or Rh increases the reducibility of the Ni catalyst, and enhances the nickel dispersion on the alumina support, and hence the number of active sites for hydrogen chemisorption.

Catalytic activity tests consisting in TPRea experiments showed that Ni/Al_2O_3 is effective in the NO + H_2 reaction, but only at T > 220°C. In this temperature domain, Ni/Al_2O_3 exhibits NO conversion values of ~95 % and N_2 selectivities over 70–80 %. Use of Pt, Pd or Rh in low loadings (0.5wt.%) as promoters in Ni/Al_2O_3 leads to an enhancement of the catalytic performance in the NO + H_2 reaction at significantly lower temperatures. Ni–Pd/Al_2O_3 is by far the most active one, as already at temperatures of 100°C and above, NO conversion of 95 % is attained, while N_2 selectivities of at least 90 % are reached at 120–125°C. Stability tests, also, showed that only Ni–Pd/Al_2O_3 exhibits stable catalytic parameters during studied TOS. These very good catalytic activity results for Ni–Pd/Al_2O_3 may be attributed to both preference for molecularly adsorption of NO on the Pd sites and the ability of Pd to form palladium hydrides, which could liberate additional hydrogen during the NO + H_2 reaction. Thus, the superior catalytic performance of Ni–Pd/Al_2O_3, together with the lower catalyst costs involved, make the Pd promoted Ni catalyst an interesting alternative for specific industrial applications, such as NOx sources with low oxygen content.

CHAPTER 5
Mathematical modeling of the deNOx reactor

This chapter describes the mathematical model developed for the experimental deNOx reactor used in the catalytic activity tests, considering the catalytic bed formed by the Pd (1wt.%)/Al_2O_3 catalyst. A 3D reactor model was built in COMSOL and used to investigate the reaction behavior and transport phenomena occurring in the free and porous regions of the reactor tube. The developed reactor model was further used for parametric studies in order to investigate the influence of several key parameters upon the catalytic performance of the reactor. Thus, parametric studies included the influence of the operating temperature, the effect of the GHSV, the influence of the NO/H_2 ratio, or of the NO concentration in the feed on the NOx conversion and N_2 yield.

5.1. Introduction

Design and development of new and efficient catalysts for a specific process involves an important volume of work and time, and consequently of financial resources, due to the large number of experiments required to characterize and test each catalyst from a series under different operating conditions. Moreover, implementation into the whole process of the best catalyst thus obtained significantly adds to the total involved costs. Under these circumstances, process modeling has gained a lot of interest in the last decades, as performance of expensive and time consuming experiments could be spared [159]. The development of process models is not intended to fully replace experimental research, but to limit it as much as possible and to complete the understanding of the process. In case of detailed modeling of a chemical process, simulations can help in understanding the specific behaviors of the process, as well as the interconnections between the various chemical and physical processes occurring in the system [160].

The aim of this chapter is the development of a mathematical model based on momentum and mass balance equations, using a mechanistic–based kinetic model in order to (i) describe and understand the flow and reaction behavior in the experimental reactor by performing steady state simulations, and to (ii) predict the reactor behavior under the variation of several operating parameters. Our approach was to integrate a kinetic model for the Pd (1wt.%)/Al_2O_3 catalyst into the reactor model, and then validate it against our experimental results obtained for the same catalyst. The validated model was then used for parametric studies in order to survey other more favorable operating conditions without affecting the catalytic performances.

5.2. Thermodynamic analysis

Thermodynamic analysis provides important information for the design and operation of a chemical reactor, such as: (i) the amount of heat absorbed or released during the chemical process, which further allows thermal design of the reactor, and (ii) the maximum conversion reachable under specific reaction conditions. Evaluation of reaction enthalpy (from thermodynamic data) leads to the following thermochemical equations:

$$NO_{(g)} + H_{2(g)} \rightarrow 0.5N_{2(g)} + H_2O_{(g)} \qquad \Delta_R H^{298} = -337.07 \text{ kJ/mol} \quad (5.4)$$

$$NO_{(g)} + 0.5H_{2(g)} \rightarrow 0.5N_2O_{(g)} + 0.5H_2O_{(g)} \qquad \Delta_R H^{298} = -170.14 \text{ kJ/mol} \quad (5.5)$$

$$NO_{(g)} + 2.5H_{2(g)} \rightarrow NH_{3(g)} + H_2O_{(g)} \qquad \Delta_R H^{298} = -378.18 \text{ kJ/mol} \quad (5.6)$$

It may be observed that the reactions considered are all exothermic, meaning that reduction of NO by hydrogen proceeds with heat release to the surroundings.

Thermodynamic calculations can also give information about the chemical equilibrium of the system, or the spontaneity of a chemical reaction. Evaluation of the Gibbs energy in the temperature range of 50–350°C (the same as for the catalytic tests) shows that, at all temperatures, these reactions are spontaneous towards the formation of the N reduced species, due to the negative values over the entire domain (Fig. 5.1).

In the context of catalytic reactions, it should be highlighted here that the catalyst does not influence the equilibrium of a reaction, but lowers the activation energy needed to reach this equilibrium. In practice, chemical processes are carried out far from the equilibrium in order to benefit as much as possible from the desired reaction. Thus, an important question arises here: how far from equilibrium is it convenient to conduct the NO reduction process? The approach–to–equilibrium (η_{eq}) is a parameter which may be successfully used in order to favor the desired reaction [161] (the reduction of NO):

$$\eta_{eq} = \frac{Q}{K} \qquad (5.9)$$

$$\Delta_R G^T = -RT \ln K + RT \ln Q = RT \ln \frac{Q}{K} = RT \ln \eta \qquad (5.11)$$

A reaction is closer to equilibrium when η approaches the value of 1, that is a reaction is farther from the equilibrium if $\ln \eta$ is more negative. Fig. 5.2 shows that all three reactions are very far from equilibrium, as $\ln \eta$ gives very large negative values over the entire temperature domain. This means that at each working temperature the forward reaction is favored, and that at atmospheric pressure, each reaction temperature is a good choice from

the thermodynamic point of view. These results allow us to assume that all three reactions are basically irreversible in the investigated experimental conditions.

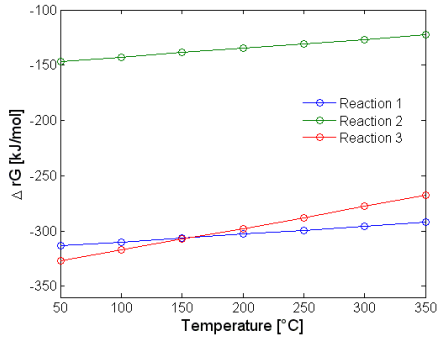

Fig. 5.1. Gibbs energy values as a function of temperature for reactions (5.4) – Reaction 1, (5.5) – Reaction 2, and (5.6) – Reaction 3.

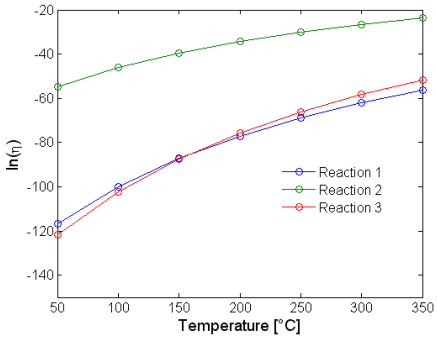

Fig. 5.2. The approach–to–equilibrium at different temperatures for reactions (5.4) – Reaction 1, (5.5) – Reaction 2, and (5.6) – Reaction 3.

5.3. Kinetic model

The kinetic model proposed and described in the following accounts for the formation and distribution of the reaction products formed during the reduction of NO by H_2 on alumina supported noble metal catalysts: N_2, N_2O, and H_2O. It should be reminded here that, in the experimental conditions explored in this work, formation of neither NH_3 nor NO_2 was evidenced. The reaction steps are listed below (S stands for a vacant catalytic site):

$$(R_1)\ NO + S \rightarrow NO_{(S)} \qquad (5.12)$$

$$(R_2)\ H_2 + 2S \rightarrow 2H_{(S)} \qquad (5.13)$$

$$(R_3)\ NO_{(S)} + H_{(S)} \rightarrow N_{(S)} + OH_{(S)} \qquad (5.14)$$

$$(R_4)\ NO_{(S)} + S \rightarrow N_{(S)} + O_{(S)} \qquad (5.15)$$

$$(R_5)\ N_{(S)} + N_{(S)} \rightarrow N_2 + 2S \qquad (5.16)$$

$$(R_6)\ NO_{(S)} + N_{(S)} \rightarrow N_2 + O_{(S)} + S \qquad (5.17)$$

$$(R_7)\ NO_{(S)} + N_{(S)} \rightarrow N_2O + 2S \qquad (5.18)$$

$$(R_8)\ NO_{(S)} + NO_{(S)} \rightarrow N_2O + O_{(S)} + S \qquad (5.19)$$

$$(R_9)\ O_{(S)} + H_{(S)} \rightarrow OH_{(S)} + S \qquad (5.20)$$

$$(R_{10})\ OH_{(S)} + H_{(S)} \rightarrow H_2O + 2S \qquad (5.21)$$

The proposed mechanism illustrates the contribution of chemisorbed hydrogen to the dissociation of molecularly adsorbed NO (eq. (5.14)). Formation of N_2, the desired reaction product, is due to either the recombination of two adjacent adsorbed N atoms (eq. (5.16)) or the combination of a molecularly adsorbed NO molecule with an adsorbed N atom previously formed (step (5.17)). On the other hand, N_2O predominantly resulted at reaction temperatures below 150°C (see Chapter 3, Fig. 3.4) is due to the recombination of either two adjacent molecularly adsorbed molecules (step (5.19)), or the combination of an adsorbed NO molecule with a N adatom (5.18). Moreover, it is assumed that formation of water according to step (5.21) is irreversible and that its desorption occurs instantaneously [96].

The rate of NO transformation into products, or the rates of the other species present in the reactor space can be established by:

$$R_{NO} = \frac{2k_3\lambda_{NO}p_{NO}\sqrt{\lambda_H p_{H_2}}}{\left(1+\lambda_{NO}p_{NO}+\sqrt{\lambda_H p_{H_2}}\right)^2} \qquad (5.33)$$

$$R_{H_2} = \frac{2k_6+k_7}{k_6+k_7}k_3\theta_{NO}\theta_H \qquad (5.35)$$

$$R_{N_2} = \frac{k_6}{k_6+k_7}k_3\theta_{NO}\theta_H \qquad (5.36)$$

$$R_{N_2O} = \frac{k_7}{k_6+k_7}k_3\theta_{NO}\theta_H \qquad (5.37)$$

$$R_{H_2O} = \frac{2k_6+k_7}{k_6+k_7}k_3\theta_{NO}\theta_H \qquad (5.38)$$

where k_6 and k_7 are the kinetic constants for reactions R_6(5.17) and R_7(5.18), respectively.

The obtained rate expression for NO is similar to the one obtained by the group of Granger [163]. It must be emphasized here that their kinetic model considered the formation of ammonia as byproduct, besides N_2 and N_2O. However, approximations used in the kinetic model of Granger et al. are equivalent to our experimental observations regarding the lack of ammonia in the effluent gases. On the other hand, the characteristics of the catalyst used by Granger et al. for kinetic analyses (BET surface area, porosity, metal dispersion, metal surface area, etc.) are similar to those corresponding to our Pd supported alumina catalyst. Therefore, kinetic constants and parameters obtained by the group of Granger (Table 5.1) will be further used for the mathematical model of the deNOx reactor.

Table 5.1. Parameters of the kinetic model [69,163].

Catalyst	A (mol/m^3/s)	E (J/mol)	f_{NO} (Pa^{-1})	f_H (Pa^{-1})	$\Delta_{ads}H^{NO}$ (J/mol)	$\Delta_{ads}H^{H}$ (J/mol)
Pd (1wt.%)/Al_2O_3	$2.69\cdot10^{13}$	$82\cdot10^{3}$ *	$7.11\cdot10^{-10}$	$3.45\cdot10^{-9}$	$-42.6\cdot10^{3}$	$-16.6\cdot10^{3}$

$k_3 = A\exp\left(-\frac{E}{RT}\right)$, $\lambda_{NO} = f_{NO}\exp\left(-\frac{\Delta_{ads}H^{NO}}{RT}\right)$, $\lambda_H = f_H\exp\left(-\frac{\Delta_{ads}H^{H}}{RT}\right)$; *value adjusted to capture the experimental trends.

However, there are no estimates of the kinetic parameters for reactions R_6(5.17) and R_7(5.18) which are needed for the evaluation of the reaction rates of all components of the system. It should be reminded here that experimental catalytic activity test showed that formation of N_2 and N_2O are temperature dependent, N_2O selectivity being increased in the lower temperature domain, i.e. at T < 100°C (see Fig. 3.4 and 3.20). Therefore, in order to illustrate this dependence, we have proposed a relationship between the corresponding kinetic constants of reactions R_6(5.17) and R_7(5.18), which satisfactory validates our experimental results. Thus, in the lower temperature domain (T < 100°C), the ratio $k_6/(k_6+k_7)$ can be approximated by $a=(T-273)/100$, where T is the reaction temperature

expressed in K, while at higher temperatures this ratio can be approximated by a factor of 0.85 considering that N_2 selectivity is practically constant in this domain.

5.3.1. Validation of the kinetic model

The validity of the proposed kinetic model against our experimental catalytic results was first checked using a MATLAB subroutine which accounts only for the reactions taking place in the catalytic bed. Evaluations of NO conversion and N_2 selectivity over the entire temperature domain (50–350°C) using the proposed kinetic model revealed a good fit with our experimental results (Fig. 5.5). Thus, it may be concluded that the proposed kinetic model is convenient for implementation into the deNOx reactor model.

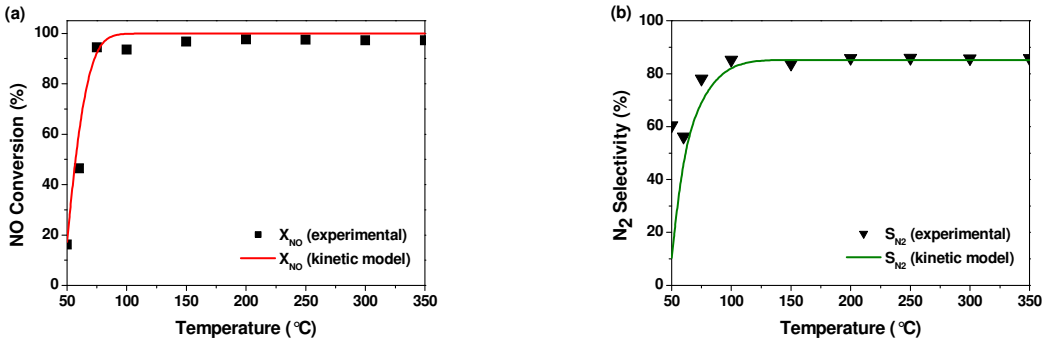

Fig. 5.5. Experimental vs. simulated NO conversion (a) and N_2 selectivity (b) profiles using the proposed kinetic model over the 50–350°C temperature domain (for Pd (1wt.%)/Al_2O_3, *GHSV* = 4,500 h^{-1}, NO/H_2 = 1:1.2, m_{cat} = 2 g, L_{bed} = 3.2 cm).

5.4. Mathematical model of the catalytic reactor

5.4.1. Choice of reactor type

Experimental catalytic tests were performed using packed–bed reactor operating under plug–flow conditions, so that the mathematical model to be further presented and discussed accounts for this experimental reactor. Operating conditions of the reactor, together with geometric details and catalyst characteristics are summarized in Table 5.2.

5.4.2. Configuration of the catalytic reactor

The reactor consists of three zones (Fig. 5.6): *zone 1* and *zone 3* are inert portions from the chemical point of view, where only transport phenomena occur, while *zone 2* consists in the catalytic bed where, apart from the corresponding transport phenomena, the chemical reactions take place. Regarding the distribution of the species, only the reactants (NO and H_2) are present in *zone 1*, while *zone 2* and *zone 3* are characterized by the presence

of both reactants and reaction products (N_2, N_2O, and H_2O), depending on the reaction conditions. However, no change in the distribution of the components occurs in *zone 3*.

5.4.3. Hypotheses of the model and governing equations

The mathematical model of the packed–bed deNOx reactor was developed based on a series of hypothesis, as presented in the following:

- gas phase reactions do not take place;
- laminar flow along each zone;
- reactions take place only in the catalytic bed (*zone 2*), on the catalyst surface;
- the reactions take place according to a Langmuir–Hinshelwood mechanism [163];
- diffusional gradients are negligible, meaning that all exposed metallic sites are accessible to the gaseous reactants [164];
- the catalyst temperature is uniform [89], taking into account that reactants concentration is considerable low so that deNOx reactors work under virtually isothermal conditions, and combined chemical and diffusional control.

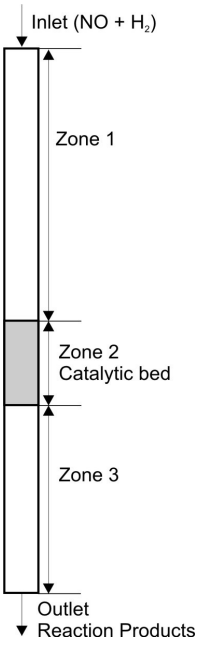

Fig. 5.6. Schematics of the deNOx reactor.

Table 5.2. Parameters of the packed–bed reactor.

Operating conditions	
NO	0.5 %
H_2	0.6 %
Ar	balance
GHSV	4,500 h^{-1}
Temperature range	50–350 °C
Pressure	101325 Pa
Catalyst Details	
Catalyst	Pd (1wt.%)/Al_2O_3
Mass	2 g
BET surface area	206 m^2/g
Porosity (ε)	0.75
Average particle size (d_p)	~0.2 mm
Reactor Geometry	
Length of catalyst bed, L_{bed}	32 mm
Length of reactor, L_R	300 mm
Reactor inner diameter	9 mm

5.4.3.1. Transport phenomena in the inert zones (zone 1 and zone 3)

The inert regions of the reactor are free channels, so that flow of the gaseous mixture, represented by either the reactants in *zone 1*, or the reaction products together with unconverted reactants in *zone 3*, is described by the Navier–Stokes equation:

$$\rho\frac{\partial u}{\partial t}+\rho(u\cdot\nabla)u=F-\nabla p+\eta\nabla^2 u \qquad (5.45)$$
$$\nabla\cdot u=0$$

Since there are no reactions in these regions, no concentration gradients occur, so that no mass balance equations are needed. Thus, the inert regions of the reactor (*zone 1* and *zone 3*) are fully described by the momentum balance equation.

5.4.3.2. Transport phenomena in the catalyst zone (zone 2)

In the catalytic bed zone, flow of the gaseous mixture occurs through a porous medium given by the employed catalyst, so that momentum equation must be corrected by the Brinkman equation which accounts for the porosity and permeability of the medium:

$$\rho\frac{\partial u}{\partial t}+\frac{\eta}{\kappa}u=F-\nabla p+\frac{\eta}{\varepsilon}\nabla^2 u \qquad (5.49)$$
$$\nabla\cdot u=0$$

The mass balance equations describing mass transport in the catalytic zone (*zone 2*) are given by the diffusion–convection equations at steady state across the reactor:

$$\nabla\cdot\left(-D_i\nabla c_i+c_i u\right)=R_i \qquad (5.52)$$

All parameters and properties needed for solving the reactor model were determined by means of the well known equations in the field of chemical – physics, and were implemented in a MATLAB subroutine (Annex 4 in the thesis).

5.4.4. Reactor model using COMSOL Multiphysics

COMSOL Multiphysics® is a dedicated software platform for modeling and simulating a multitude of scientific and engineering problems, by means of advanced numerical methods [168]. One of the most important features of COMSOL is the ability to couple several physics into an integrated model, and thus to solve multiphysics phenomena.

A 3D reactor model was built considering a cylindrical geometry of the reactor, and accounting for the exact position of the catalyst bed inside the reactor tube. In order to account for the model equations presented above, two physics from the COMSOL physics library were considered: (1) the Free and Porous Media Flow Interface (*fp*); and (2) the Transport of Diluted Species Interface (*chds*). Unless otherwise specified, simulation studies were performed using Coarser mesh for the entire geometry, and the Direct (MUMPS) solver, under the error control of a 10^{-3} relative tolerance.

5.5. Simulation results

5.5.1. Flow behavior in the tubular reactor

Simulations of the 3D reactor model showed that the variation of pressure in the experimental deNOx reactor occurs mainly in the porous region, represented by the catalytic bed (Fig. 5.9), while pressure drop does not exceed 0.03 % of the total pressure in the reactor, at the highest evaluated temperature.

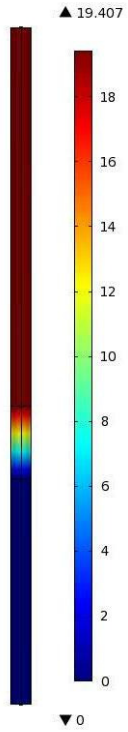

Fig. 5.9. Pressure drop across the reactor at 100°C.

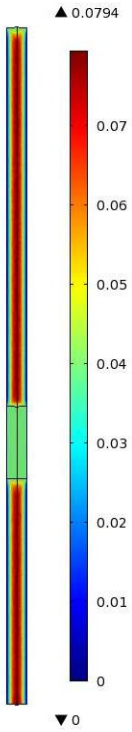

Fig. 5.10. Velocity field in the free and porous regions.

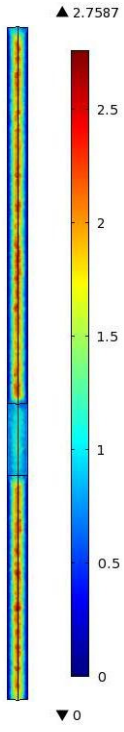

Fig. 5.11. Reynolds number across the reactor.

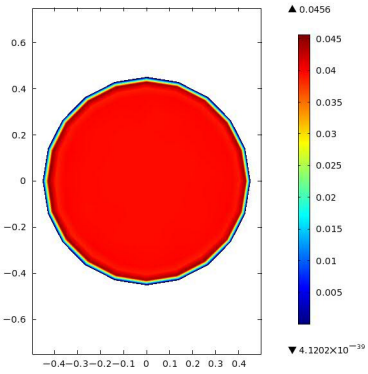

Fig. 5.12. Velocity field at the catalyst bed outlet section (y_{bed} = 3.2 cm).

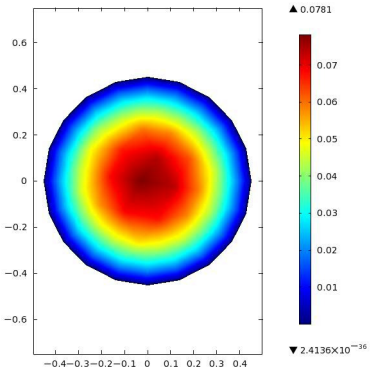

Fig. 5.13. Cross–sectional velocity field at the reactor tube outlet.

The gas velocity profiles obtained at each simulated temperature show that flow in the porous region of the reactor is almost homogeneous, while in the free regions a laminar flow

profile is developed (Fig. 5.10). Indeed, the low Reynolds numbers obtained ($Re < 1$) confirm the hypothesis of laminar flow stated above (Fig. 5.11). Cross–sectional velocity profiles at different positions of the reactor tube show that the velocity magnitude is practically constant over almost the entire section of the reactor in the catalytic zone (Fig. 5.12), while after exiting the catalyst bed, flow of the gaseous mixture is fully developed under laminar conditions (Fig. 5.13).

5.5.2. Reaction behavior in the catalyst bed

Considering the reactions of interest, steady state simulation results for the 3D reactor model are in good agreement with the experimental results, at each temperature. However, slightly superior NO conversion values were obtained by simulations. Thus, at 100°C simulations show a value around 99 %, compared to 94 % experimentally obtained, while at 150°C, total NO conversion is obtained by simulation, compared to 97 %, experimentally. In respect to N_2 selectivity, simulations showed values around 85 %, while, experimentally, selectivity values of 85.3 % at 100°C and 83.8 % at 150°C were calculated.
Besides the agreement with the experimental results, the reactor model revealed the catalyst behavior during the reduction of NO by hydrogen. It is interesting to observe that already at 100°C, NO is reduced by hydrogen rapidly after the feed enters the catalytic bed. Fig. 5.14 (a) shows that reduction of NO occurs in the first half of the catalyst bed, while Fig. 5.14 (b) demonstrates that, at 100°C, final NO conversion is attained at this position, that is $y_{bed} = 1.6$ cm. Figures 5.16 and 5.17 illustrating the NO concentration fields at the inlet of the catalyst bed and at half of the catalyst bed length, respectively, confirm that NO is practically completely converted by the middle of the porous medium. These results suggest that the catalyst bed is not conveniently used for the reduction of NO by hydrogen, and that the length of the catalyst bed could be reduced for these reaction conditions. Moreover, simulation results obtained for higher reaction temperatures enforce the idea of improper use of catalyst during the experimental tests. Thus, at 150°C, for example, the conversion of NO into reaction products occurs more rapidly, that is in the first quarter of the catalyst bed length (figure not shown here). Regarding the distribution of N_2 into the catalytic bed, simulations did not reveal any significant differences between the results obtained at each of the tested temperature. Thus, for example, at 100°C, simulations show that N_2 is formed rapidly after the feed enters the catalytic zone (Fig. 5.15 (a)). Consequently, N_2 selectivity profile along the catalyst bed shows values in a narrow range, as S_{N2} increases rapidly to the final value (Fig. 5.15 (b)). It should be reminded here that, except for the reactor outlet

values of the different parameters, their distribution along the reactor or catalyst bed cannot be compared to experimental results, as catalytic tests did not reveal any 'inside' behavior.

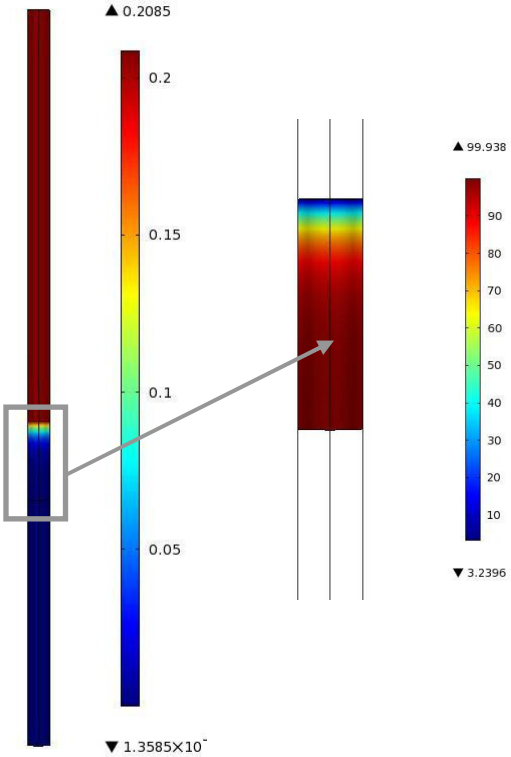

(a) **(b)**

Fig. 5.14. (a) NO concentration profile along the reactor and (b) NO conversion profile along the catalyst bed, at 100°C.

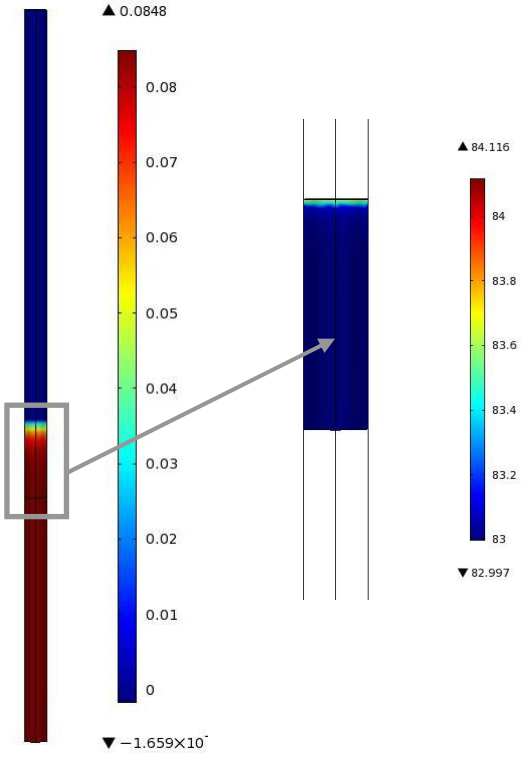

(a) **(b)**

Fig. 5.15. (a) N_2 concentration profile along the reactor and (b) N_2 selectivity profile along the catalyst bed, at 100°C.

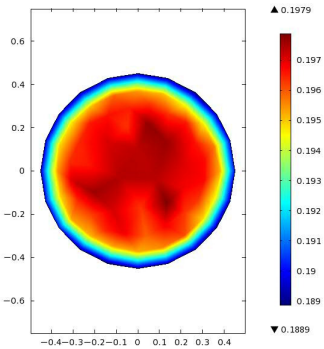

Fig. 5.16. NO concentration field at the entrance into the catalytic bed, at 100°C.

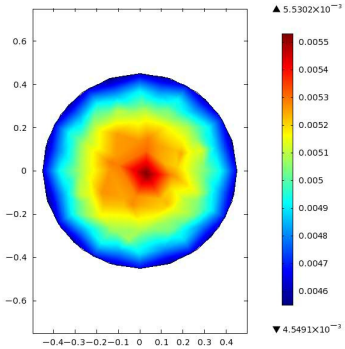

Fig. 5.17. NO concentration field at half of the catalyst bed ($y_{bed} = 1.6$ cm), and at 100°C.

Simulation results revealed a surprising behavior of the catalyst in the deNOx reaction. It was unexpected that reactants are rapidly converted into reaction products after the feed enters the catalyst, in other words that only half, at the most, from the available catalytic material is actually involved in the reduction of NO. However, somehow similar observations were revealed by simulations of a 3D reactor model involving NO reduction by

ammonia, and not hydrogen, performed by Chen and Tan [93]. Indeed, their optimized reactor model for NH_3–SCR also showed that soon after entering the catalytic zone, NO is converted into products. It should be emphasized here that this is not a straightforward comparison, mostly because the reaction conditions reported in the work of Chen and Tan are different from ours, the most important being the reducing agent (NH_3, and not H_2), and the reaction mechanism involved (Eley–Rideal, and not Langmuir–Hinshelwood).

5.6. Parametric studies

For the purpose of parametric studies, a 2D reactor model was employed in order to reduce the high simulation times needed to run parametric sweeps on the 3D reactor model. The 2D reactor model is completely identical to the 3D one, except for the dimensions. Therefore, tests were performed in order to exclude differences in simulation results due to running a 2D model instead of the 3D reactor model. No differences were observed in any of the evaluated parameters obtained by the 2D reactor model compared to the 3D model.

5.6.1. Effect of reaction temperature

In the parametric sweep involving the reaction temperature, simulations were performed by variation of this parameter in the range of 50 to 350°C (consistent with the experimentally tested temperature domain), by steps of 10 degrees. Simulation results show that changes in the concentration distribution of either of the systems' components occur only after the feed enters the catalytic bed, while after the gaseous flux exits the catalyst no further modifications are to be noticed (Fig. 5.24 and 5.25). Concentration profiles of the components (NO and N_2 presented here in Fig. 5.24 and 5.25, respectively) reveal that the most important differences occur at $T < 100$°C. Thus, temperature increase by each 10 degrees in this narrow domain leads to significant decreases regarding the concentration of NO, and the consequent large increases of the N_2 concentration. Also, it should be noticed that already at 90°C, final NO or N_2 concentration is reached within the catalyst bed, shortly before exiting the catalytic zone, proving thus that the length of the catalyst bed is sufficient for the conversion of NO to N_2 starting with this temperature value. On the other hand, concentration profiles obtained at temperature values above 100°C are almost identical, and final concentration values are reached by the half of the catalyst bed length. A closer look upon the catalyst behavior reveals that conversion profiles along the catalyst bed for both reactants (NO and H_2) are strongly influenced by T (see Fig. 5.26 and 5.27). Conversion profiles for both reactants emphasize that reaction temperatures above 100–150°C do not

lead to better conversion values for either NO or H_2. These simulation results are consistent with the experimental results for the Pd (1wt.%)/Al_2O_3 catalyst. In respect to the reaction product of interest, simulation results due to temperature parametric sweep reveal that N_2 yield profiles are quite similar to the reactants' conversion profiles (figure not shown here). Maximum N_2 yields of ~85 % are attained already at 90–100°C, consistent with the experimental results (Fig. 3.21).

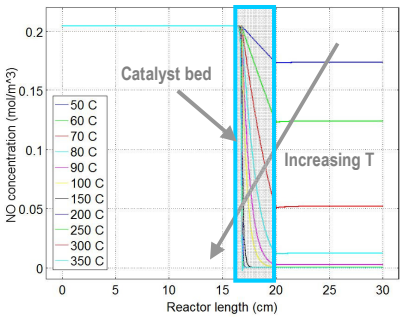

Fig. 5.24. NO concentration profiles along the reactor tube, at different T ($GHSV$ = 4,500 h^{-1}, NO/H_2 = 1:1.2, $[NO]^{in}$ = 0.5 %, L_{bed} = 3.2 cm).

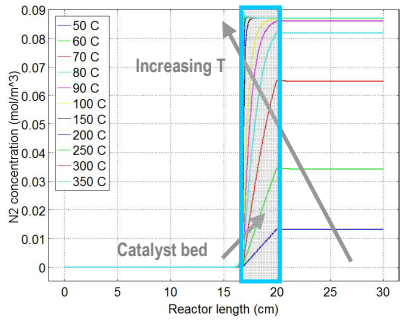

Fig. 5.25. N_2 concentration profiles along the reactor tube, at different T ($GHSV$ = 4,500 h^{-1}, NO/H_2 = 1:1.2, $[NO]^{in}$ = 0.5 %, L_{bed} = 3.2 cm).

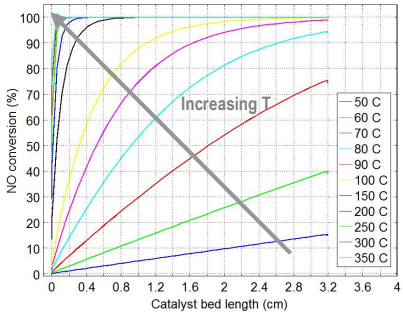

Fig. 5.26. NO conversion profiles along the catalyst bed, at different T ($GHSV$ = 4,500 h^{-1}, NO/H_2 = 1:1.2, $[NO]^{in}$ = 0.5 %, L_{bed} = 3.2 cm).

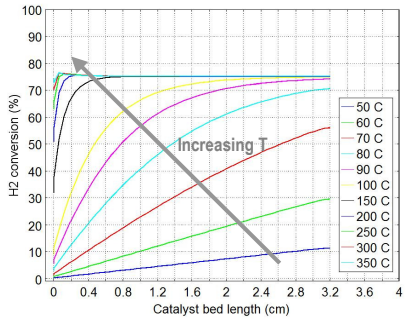

Fig. 5.27. H_2 conversion profiles along the catalyst bed, at different T ($GHSV$ = 4,500 h^{-1}, NO/H_2 = 1:1.2, $[NO]^{in}$ = 0.5 %, L_{bed} = 3.2 cm).

5.6.2. Effect of *GHSV*

Considering the definition of the gas hourly space velocity (*GHSV*) as the ratio between the volumetric flow rate of the feed and the catalyst volume, it can be noticed that variation of this parameter is achieved either by varying the feed flow rate or the catalyst volume. Both approaches will be presented and discussed in the followings.

5.6.2.1. Variation of feed flow rate

In order to study the influence of the *GHSV* upon the reactor performance by varying the feed rate, values of the reactants inlet flow were selected in the range of 60 to 360 mL/min, by steps of 30 mL/min, corresponding to *GHSVs* in the 1,800–10,800 h^{-1} domain.

At 150°C, simulation results at different *GHSVs* (obtained by feed variation) show that concentration profiles of each component are almost identical along the reactor tube (Fig. 5.30 for NO). A closer insight into the catalyst behavior reveals that, at this temperature, variation of the *GHSV* values does not significantly influence the NO conversion profiles along the catalytic zone (Fig. 5.32.). Thus, by increasing *GHSV*, conversion of NO is slightly decreased up to the half of the catalyst bed length. However, final conversion values at the catalyst bed exit are identical, regardless of the *GHSV* value used. N_2 yield profiles, also, reveal no significant differences along the catalyst bed (simulation results not presented here). These results imply that larger feed rates of NOx containing effluent gases can be efficiently treated at 150°C using the Pd (1wt.%)/Al_2O_3 catalyst.

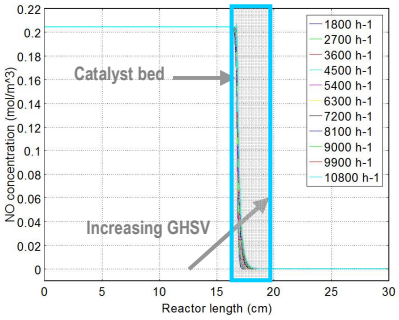

Fig. 5.30. NO concentration profiles along the reactor tube, at different *GHSV* (T = 150°C, NO/H_2 = 1:1.2, $[NO]^{in}$ = 0.5 %, L_{bed} = 3.2 cm).

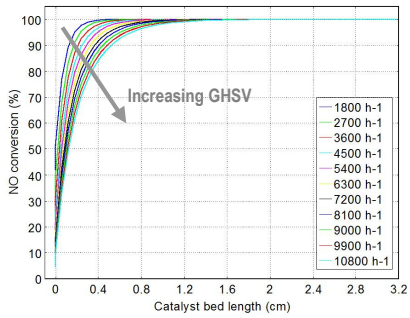

Fig. 5.32. NO conversion profiles along the catalyst bed, at different values of *GHSV* (T = 150°C, NO/H_2 = 1:1.2, $[NO]^{in}$ = 0.5 %, L_{bed} = 3.2 cm).

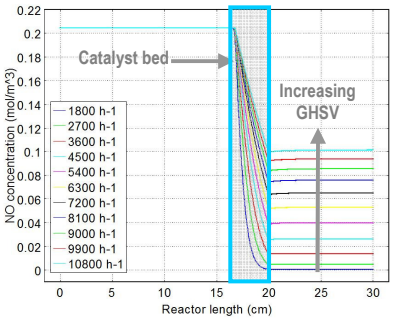

Fig. 5.34. NO concentration profiles along the reactor tube, at different *GHSVs* (T = 75°C, NO/H_2 = 1:1.2, $[NO]^{in}$ = 0.5 %, L_{bed} = 3.2 cm).

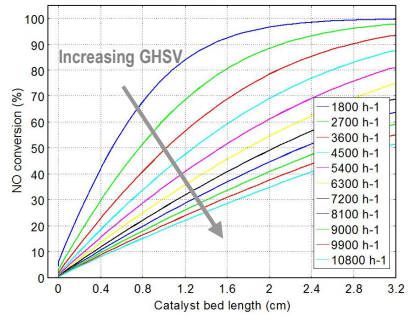

Fig. 5.36. NO conversion profiles along the catalyst bed, at different *GHSVs* (T = 75°C, NO/H_2 = 1/1.2, $[NO]^{in}$ = 0.5 %, L_{bed} = 3.2 cm).

More interesting simulation results due to *GHSV* variation were obtained at lower reaction temperatures, e.g. 75°C. Increasing feed rates (and thus increasing *GHSVs*) lead to larger final NO concentration values and consequent lower N_2 concentration values (Fig.s 5.34), proving thus the detrimental effect of larger *GHSVs* upon the NOx removal efficiency at this temperature. On the other hand, concentration profiles for both NO and N_2 reveal that at lower *GHSVs*, i.e. 1,800 h^{-1}, the catalyst bed length is well used in the reaction, so that NO is

completely reduced by H_2 already before the gases exit the catalytic zone. An insight into the catalytic zone reveals that, even at this low reaction temperature (75°C), total NO conversion can be reached at the lowest *GHSV* (1,800 h^{-1}) by the last quarter of the catalyst bed length (Fig. 5.36), suggesting that lower temperatures are a good alternative for total NO removal in case lower feed rates of effluent gases. Fig. 5.38 illustrates the effect of the *GHSV* on the conversion of NO evaluated at catalyst bed exit (*not* along the catalytic zone) as a function of temperature. Thus, regardless of the *GHSV* value, total NO conversion can be achieved at temperatures above 125°C, while very low *GHSVs* (i.e. 1,800 or even 3,600 h^{-1}) ensure very high NO conversions even in the lower temperature domain (75–125°C).

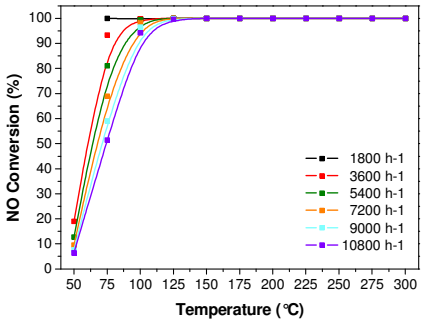

Fig. 5.38. *GHSV* influence on the NO conversion at catalyst bed outlet under different operating temperatures (NO/H_2 = 1:1.2, $[NO]^{in}$ = 0.5 %, L_{bed} = 3.2 cm).

5.6.2.2. Variation of catalyst volume

Taking into account that variation of *GHSV* actually implies a change of the gas mixture velocity, it results that variation of this parameter due to catalyst volume can only be achieved by varying the cross–sectional area of the reactor tube, and not the catalyst bed length for a selected feed rate. Thus, simulations were performed by varying the diameter of the reactor tube from 0.4 cm to 3 cm by 0.2 cm steps, which result in the consequent variation of the cross–sectional area.

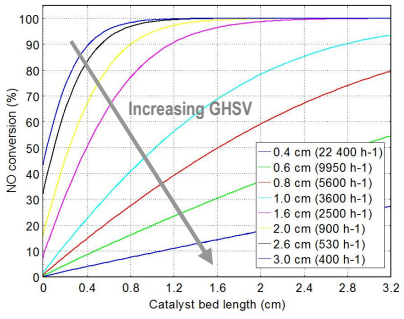

Fig. 5.39. Effect of reactor diameter on the NO conversion along the catalyst bed (T = 75°C, NO/H_2 = 1:1.2, $[NO]^{in}$ = 0.5 %, L_{bed} = 3.2 cm).

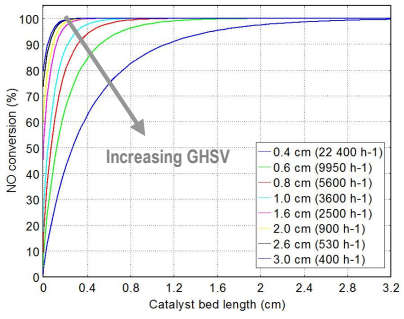

Fig. 5.40. Effect of reactor diameter on the NO conversion along the catalyst bed (T = 150°C, NO/H_2 = 1:1.2, $[NO]^{in}$ = 0.5 %, L_{bed} = 3.2 cm).

Figures 5.39 and 5.40 show that increasing the *GHSV* leads to lower NO conversion values, similar to the case discussed in Section 5.6.2.1. More importantly, it should be noticed that regardless of the approach to vary the *GHSV* (either by feed variation or reactor geometry modification), similar catalytic performance parameters are obtained for a specific *GHSV* value. It results that depending on the process limitations, one can choose one of these two approaches in order to obtain a certain *GHSV* value.

5.6.3. Effect of NO/H_2 ratio

The reactants ratio in the feed is important from two perspectives: (i) NO should be totally reduced and converted to N_2 to the largest extent; and (ii) use of unnecessary excess of reducing agent should be avoided. In order to evaluate the effect of $NO/H_2 = 1/r$ on the catalytic performance, simulations were carried out by varying r from 0.8 to 2.0, by steps of 0.2. At 150°C, except for the ratio of 1/0.8 when only 89 % of NO was converted, in all other cases total NO conversion was achieved by the first quarter of the catalytic zone (Fig. 5.41). Hydrogen, on the other hand, is totally converted only in the case when it is the limiting reactant in the system (NO/H_2 = 1/0.8) (Fig. 5.42). It is interesting to observe that already for NO/H_2 = 1/1.0, NO is totally converted, with a corresponding H_2 conversion of 90 % and also with maximum N_2 yield (Fig. not shown here). These results suggest that in case of Pd (1wt.%)/Al_2O_3 the reactants ratio could be reduced from 1/1.2, as used experimentally, to 1/1.0, and still have total NO conversion. Fig. 5.46 summarizes the effect of simultaneous variation of T and NO/H_2 ratio, from the perspective of reactants conversion at catalyst bed exit. It results that for a stoichiometric ratio or above, a temperature range of 100 – 150°C ensures total NO conversion. Below 100°C down to 75°C, conversion of NO varies between 80 and 98 %, directly proportional to the reactants ratio used. The extent of H_2 conversion decreases with increasing NO/H_2 ratio, maximum values for each ratio being attained at least starting with 100°C (Fig. 5.46 (b)).

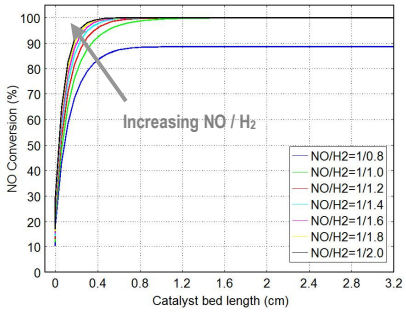

Fig. 5.41. Effect of NO/H_2 on NO conversion along the catalyst bed
(T = 150°C, $GHSV$ = 4500 h^{-1}, $[NO]^{in}$ = 0.5 %).

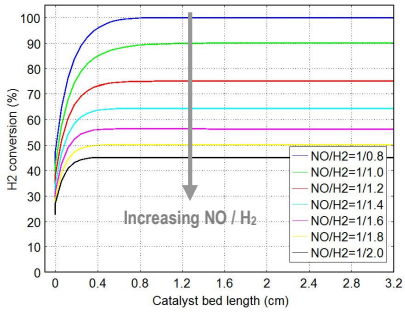

Fig. 5.42. Effect of NO/H_2 on H_2 conversion along the catalyst bed
(T = 150°C, $GHSV$ = 4500 h^{-1}, $[NO]^{in}$ = 0.5 %).

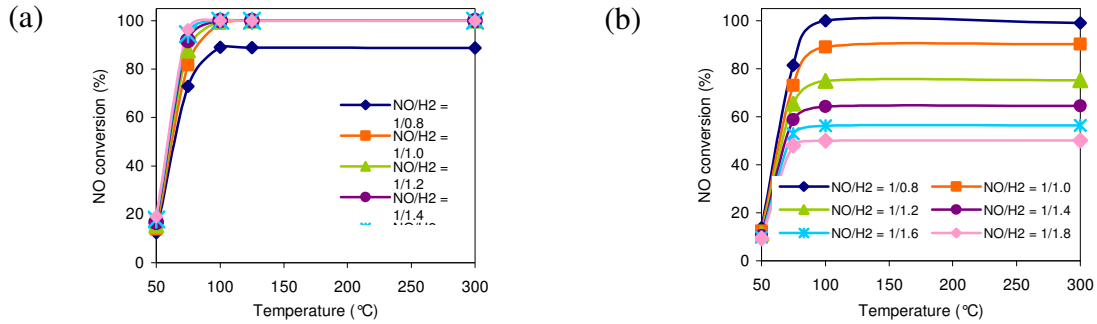

Fig. 5.46. The effect of NO/H_2 on the conversion of (a) NO, and (b) H_2, under different operating temperatures ($GHSV$ = 4,500 h^{-1}, $[NO]^{in}$ = 0.5 %, L_{bed} = 3.2 cm).

5.6.4. Effect of inlet NO concentration

One of the goals in developing a new technology is to achieve as much flexibility as possible in using it. Thus, for the specific case of NO abatement by reduction with H_2, if the selected catalyst would be efficient in the treatment of various NO concentrations in the feed, this would lead to operating flexibility of the process. For this purpose, the developed reactor model was used to run a parametric study involving the variation of $[NO]^{in}$ from 0.1 % to 1.0 %, by steps of 0.1 %, and keeping all other operating parameters constant. At 150°C, regardless of the concentration in the feed, NO is totally converted by the half of the catalyst bed length, at the most (Fig. 5.47 (a)). At 75°C, on the other hand, Fig. 5.47 (b) shows that NO conversion increases slowly along the catalytic zone for each $[NO]^{in}$ value, while NO conversion values at catalyst bed exit are in the range of 78–88 %.

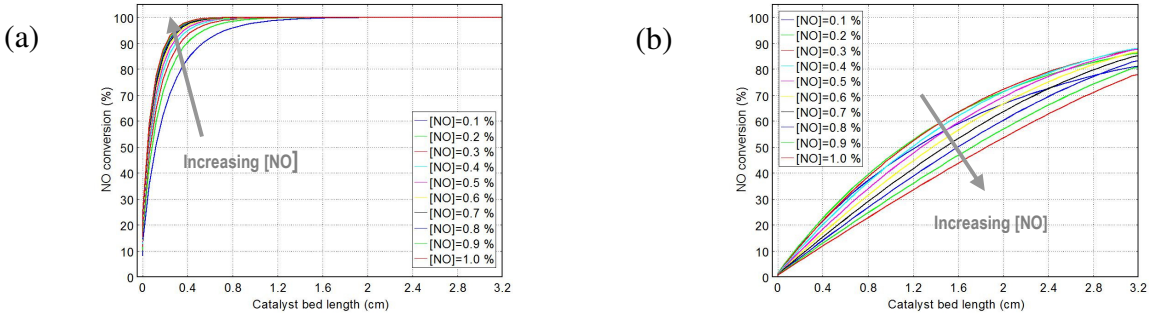

Fig. 5.47. Simulated NO conversion profiles along the catalyst bed for different concentrations of NO in the feed: (a) T = 150°C, and (b) T = 75°C ($GHSV$ = 4,500 h^{-1}, NO/H_2 = 1.2, L_{bed} = 3.2 cm).

Fig. 5.48 illustrates the effect of simultaneous variation of both $[NO]^{in}$ and T, on the conversion of NO at catalyst bed outlet. Thus, irrespective of the $[NO]^{in}$, practically total conversion of NO could be reached in the temperature range of 100 to 150°C, with only slightly lower value at 100°C and $[NO]^{in}$ = 0.1 %. These simulation results are consistent

with the experimental results: a narrow temperature window of 100–150°C is sufficient for total NO conversion with maximum N_2 yield, for a large range of $[NO]^{in}$.

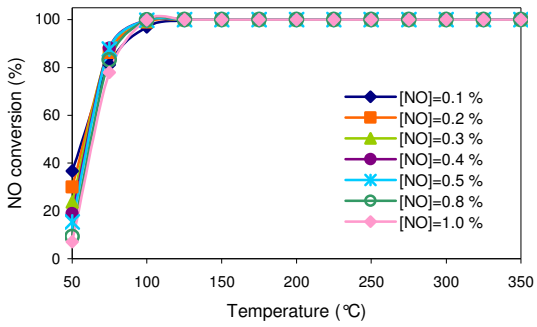

Fig. 5.48. Effect of NO concentration in the feed on the conversion of NO at catalyst bed outlet, under different operating temperatures ($GHSV$ = 4,500 h^{-1}, NO/H_2 = 1:1.2, L_{bed} = 3.2 cm).

5.7. Conclusions

The reactor used experimentally for the investigation of NO reduction by H_2 was considered for developing a comprehensive reactor model. Steady state simulations of the 3D reactor model built in COMSOL, in the conditions used in catalytic tests, revealed a good agreement with our experimental results. A more interesting observation was, however, the fact that for the experimental conditions employed in case of the Pd (1wt.%)/Al_2O_3 catalyst, at T > 100°C, the catalytic bed was not efficiently used in laboratory tests, considering that total NO conversion is reached by the half of the catalyst bed length. The most important conclusion resulted from parametric sweeps is that the narrow temperature window between 100 and 150°C is sufficient for total NO conversion and maximum N_2 yield of 85 %, irrespective of the employed *GHSVs,* the concentration of NO in the feed or the reactants ratio. Moreover, parametric studies indicate on some possibilities to lower the reaction temperature, without affecting the catalytic performances. However, in order to correctly discriminate between the effects of these parameters on the reactor performance, and also on the possible benefits (energy efficiency, total operation costs, etc), optimization procedures should be employed. It must be reminded here that in case of the reactants ratio influence on the reactor performances, simulation results should be critically considered, mostly because under excess H_2 in the feed, NO could be reduced to NH_3 also, besides N_2 and N_2O accounted for in the reaction mechanism. Finally, a very important feature of the developed reactor model is its flexibility in being used for other catalysts. Thus, as long as an adequate kinetic model is available, this could be integrated into the reactor model, and be further used for reactor design or control purposes.

CHAPTER 6

General Conclusions and Future Perspectives

The aim of this thesis was to explore a possible solution for the abatement of NOx emitted during operation of the ^{15}N separation plant by: (1) investigation and design of inexpensive catalysts with good catalytic performances (high NO conversion, very good selectivity towards N_2, good stability in time) for the reduction of NOx under low operating temperatures and without adding a new pollutant into the system (i.e. NH_3); and (2) development of a mathematical model for the catalytic reactor used in the deNOx process. The most important conclusions and contributions of the thesis are:

Objective 1

- Catalytic activity tests performed using the Pd (2wt.%)/Al_2O_3 catalyst aimed at finding the best reaction conditions for the reduction of NO by hydrogen. It was concluded that the best experimental conditions for the efficient removal of NOx from exhaust gases, irrespective of the NO concentration in the feed, are: temperature domain of 150–180°C, reactants ratio NO/H_2 in the range 1.0–1.4 (that is a small excess of hydrogen in the feed), and *GHSV* values in the lower region (3,000–7,000 h^{-1}). Temperature programmed desorption of reactants, on the other hand, revealed that both NO and H_2 are chemisorbed on the catalytic surface at ambient temperature, as well as at higher temperatures, but with different behaviors. NO–TPD experiments revealed a different adsorption mechanism for NO as a consequence of the adsorption temperature used: at 25°C NO is adsorb dissociatively to a greater extent, at 150°C molecular adsorption is predominant. In both cases, however, adsorption of NO is followed by desorption of NO, N_2, N_2O, O_2 and very low amounts of NO_2.
- For Pt (1wt.%)/Al_2O_3, Pd (1wt.%)/Al_2O_3, and Rh (1wt.%)/Al_2O_3, catalysts with lower noble metal loadings (i.e. 1wt.%), catalytic activity tests in the form of temperature programmed reactions under the reaction conditions previously established (*GHSV*, NO/H_2) revealed that both Pt and Pd catalyst have a similar behavior in respect to NO conversion: ~90 % already at 75°C, while in the temperature range of 100–150°C, slightly superior values for the Pd catalysts were obtained. If N_2 selectivity is considered, Pd (1wt.%)/Al_2O_3 shows the best values over the entire temperature range. Rh (1wt.%)/Al_2O_3 shows good catalytic performances only at T > 200°C. Thus in the investigated series the catalytic performance decreases in the order Pd (1wt.%)/Al_2O_3 >

Pt (1wt.%)/Al_2O_3 >> Rh (1wt.%)/Al_2O_3. Stability tests also confirmed the *Pd catalyst* as the most efficient one in the series for the reduction of NO by hydrogen. Both H_2–TPD and NO–TPD revealed that the investigated noble metals adsorb either hydrogen or NO. However, different patterns were observed: Pt is the most active metal for the adsorption–desorption of H_2, followed by Pd, and then Rh, while in respect to NO, both molecular and dissociative adsorption was observed in case of each catalyst.

- To the best of our knowledge, catalysts in the series Ni(10wt.%)–Pt(0.5wt.%)/Al_2O_3, Ni(10wt.%)–Pd(0.5wt.%)/Al_2O_3, and Ni(10wt.%)–Rh(0.5wt.%)/Al_2O_3 were investigated for the first time in the reduction process of NO by hydrogen. Catalytic activity tests consisting in temperature programmed reactions showed that Ni/Al_2O_3 is efficient in the reduction of NO by hydrogen only at temperatures above 220°C, with NO conversion values of ~95 % and N_2 selectivities over 70–80 %. Use of Pt, Pd or Rh in low loadings (0.5wt.%) as promoters in Ni/Al_2O_3 leads to an enhancement of the catalytic performance in the NO + H_2 reaction, at significantly lower reaction temperatures: NO is converted to a greater extent, with a much better selectivity towards the formation of N_2. In the bimetallic catalyst series, Ni–Pd/Al_2O_3 is by far the most active one. Already at temperatures of 100°C and above, NO conversion of 95 % is attained, while N_2 selectivities of at least 90 % are reached at 120–125°C. Stability tests, also, evidenced that only Ni–Pd/Al_2O_3 exhibits stable catalytic parameters during studied time on stream.
- TPR and H_2–TPD measurements proved that promotion by Pt, Pd or Rh increases the reducibility of NiO, enhances the dispersion of Ni on the alumina support, and consequently the number of active sites for hydrogen chemisorption. Also, NO–TPD analyses demonstrated that NO chemisorption capacity is enhanced in case of bimetallic catalysts, compared to Ni/Al_2O_3, either for the molecular adsorption path (T < 300°C) or for the dissociative adsorption path (T > 300°C) which leads to the desorption of N_2, N_2O, and NO_2.
- The most important contribution of the thesis in respect to the development of efficient and inexpensive catalysts for the reduction of NO by hydrogen is given by the Ni–Pd/Al_2O_3 catalyst, which exhibits very good catalytic activity performances in the lower temperature domain (100–130°C), and also good stability in time. Moreover, this catalyst is the most inexpensive catalyst in the investigated series (except for Ni(10wt.%)/Al_2O_3). Thus, for the specific case of the ^{15}N separation plant at INCDTIM, which evolves NOx containing exhaust gases with low oxygen content, the Ni–Pd/Al_2O_3 catalyst could be a viable alternative.

Objective 2

- A mathematical model was developed for the experimental deNOx reactor used in the catalytic activity tests, considering the catalytic bed formed by the Pd (1wt.%)/Al_2O_3 catalyst. This model was used for two purposes: (a) to describe and understand the flow and reaction behavior in the experimental reactor; and (b) to predict the reactor behavior under the variation of several operating parameters.
- Steady state simulations carried out with the 3D model developed using COMSOL Multiphysics are in good agreement with our experimental results: NO conversion and N_2 yield. However, simulations results revealed a very interesting behavior inside the catalytic bed, which could not be evidenced by experimental techniques: at reaction temperatures above 100°C, simulations showed that the catalytic bed was not efficiently used in laboratory tests for the Pd (1wt.%)/Al_2O_3 catalyst, as total NO conversion is reached by the half of the catalyst bed length. Simulations also showed that flow in the catalytic bed is almost homogeneous, while in the free regions a laminar flow profile is developed.
- The validated reactor model was used to carry out parametric studies in order to study the influence of several operating parameters on the reactor's behavior. It must be reminded here that the Pd (1wt.%)/Al_2O_3 catalyst was tested experimentally only under the selected best operating conditions obtained in the laboratory, so that parametric studies complete the understanding of the reactor's behavior. The most important conclusion derived from the performed parametric studies is that the narrow temperature window between 100 and 150°C is sufficient for total NO conversion and maximum N_2 yield of 85 %, irrespective of the employed *GHSVs,* the concentration of NO in the feed or the reactants ratio. On the other hand, parametric studies point out some situations in which lower reaction temperatures could be used, without affecting the catalytic performances.
- A very important feature of the developed reactor model is its flexibility in being used for other catalysts. Thus, as long as an adequate kinetic model is available, this could be integrated into the reactor model, and be further used for reactor design or control purposes.

The results presented and discussed in this thesis were published in five papers [61, 102–104, 127], while a sixth one is under preparation (also see the list of papers and presentations at international conferences, in the field of the thesis).

Dissemination in the field of the thesis

Published ISI Articles and Conference Papers

1. **M. Mihet,** M.D. Lazar – "Effect of Pd and Rh promotion on Ni/Al_2O_3 for NO reduction by hydrogen for stationary applications", *Chem. Eng. J*. **2014**, 251, 310–318.
2. **M. Mihet**, M.D. Lazar, G. Borodi, V. Almasan – "Effect of Pt Promotion on Ni/Al_2O_3 for the Selective Catalytic Reduction of NO with Hydrogen", *AIP Conf Proc*, **2013**, *1565*, 126–132.
3. **M. Mihet**, M.D. Lazar, V. Almasan, V. Mirel – „H_2–SCR at low temperatures on noble metal supported catalysts", *AIP Conf Proc*, **2012**, *1425*, 73–76.
4. **M. Mihet**, M.D. Lazar, V. Almasan, G. Borodi – "Low temperature hydrogen selective catalytic reduction of NO on Pd/Al_2O_3", *Rev. Roum. Chim*, **2011**; 56(6): 659–665.
5. **M. Mihet,** M. Lazar, V. Almasan **–** "Mobility of hydrogen species on Ni supported catalysts", *J. Phys: Conf. Ser.* 182, **2009**, 012051.

Article in preparation

M. Mihet, V.–M. Cristea, M. D. Lazar, A–M Cormos, P.S. Agachi – „Reduction of NO by hydrogen on Pd/Al_2O_3 in a plug flow reactor: experimental vs. mathematical modeling approach"

Presentations at International Conferences

1. **M. Miheț**, V.–M. Cristea, A–M Cormos, M. D. Lazăr, P.S. Agachi – „*Mathematical modeling of a fixed bed catalytic reactor for the reduction of NO by H_2"*, 2nd International Conference on Chemical Engineering, Innovative Materials and Processes, ICCE 2014, Iasi, Romania, 5–7 November **2014** (poster presentation).
2. **M. Miheț**, M. D. Lazăr, G. Borodi, V. Almăşan – „*Effect of Pt Promotion on Ni/Al_2O_3 for the Selective Catalytic Reduction of NO with Hydrogen"*, International Conference on Processes in Isotopes and Molecules, PIM 2013, Cluj–Napoca, Romania, 25–27 September **2013** (poster presentation).
3. **M. Mihet**, M.D. Lazăr, V. Almăşan, – *"Influence of Noble Metal Addition to Ni/Al_2O_3 for H_2–SCR",* 11th European Congress on Catalysis "EuropaCat 11", Lyon, France, 1 – 6 September **2013** (poster presentation).
4. **M. Miheț,** M. D. Lazăr, P. Mărginean, V. Almăşan – "*Hydrogen mobility on bimetallic Ni–Noble Metal/Al_2O_3 catalysts",* International Symposium of the Romanian Catalysis Society, RomCat 2013, Cluj–Napoca, Romania, 29–31 May **2013** (poster presentation).
5. **M. Miheț**, M. D. Lazăr, V. Almăşan, V. Mirel – „*H_2–SCR at low temperatures on noble metal supported catalysts"*, International Conference on Processes in Isotopes and Molecules, PIM 2011, Cluj–Napoca, Romania, 29 September–1 October **2011** (oral presentation).
6. **M. Miheț,** M. D. Lazăr, Gh. Borodi, V. Almăşan – "*H_2–SCR of NO on Pt/Al_2O_3 and Pd/Al_2O_3 catalysts at low temperatures"*, 10th European Congress on Catalysis "EuropaCat 10", Glasgow, Scotland, 28 August – 2 September **2011** (poster presentation).
7. **M. Miheț,** M. D. Lazăr, V. Almăşan, G. Borodi – „*Low temperature hydrogen selective catalytic reduction of NO on Pd/Al_2O_3",* International Symposium of the Romanian Catalysis Society, RomCat 2010, Iaşi, Romania, 23–26 June **2010** (poster presentation).
8. **M. Miheț**, M. D. Lazăr, V. Almăşan – „*Mobility of hydrogen species on Ni supported catalysts"*, International Conference on Processes in Isotopes and Molecules, PIM 2009, Cluj–Napoca, Romania, 24–26 September **2009** (oral presentation).

REFERENCES (selected)

[1] D. Axente, M. Abrudean, A. Baldea, Separarea izotopilor ^{15}N, ^{18}O, ^{10}B, ^{13}C prin schimb izotopic, Casa Cărții de Știință, Cluj-Napoca, 1994.

[2] K. Skalska, J.S. Miller, S. Ledakowicz, Trends in NO abatement: a review, Sci. Total Environ. 408 (2010) 3976–3989.

[4] V. Vestreng, L. Ntziachristos, A. Semb, S. Reis, I.S.A. Isaksen, L. Tarrason, Evolution of NO_x emissions in Europe with focus on road transport control measures, Atmos. Chem. Phys. 9 (2009) 1503–1520.

[7] S. Roy, M.S. Hegde, G. Madras, Catalysis for NO_x abatement, Appl. Energy. 86 (2009) 2283–2297.

[9] G. Qi, R. Yang, F. Rinaldi, Selective catalytic reduction of nitric oxide with hydrogen over Pd-based catalysts, J. Catal. 237 (2006) 381–392.

[10] P. Granger, V.I. Parvulescu, Catalytic NO_x abatement systems for mobile sources: from three-way to lean burn after-treatment technologies., Chem. Rev. 111 (2011) 3155–207.

[15] P. Forzatti, Present status and perspectives in de-NO_x SCR catalysis, Appl. Catal. A Gen. 222 (2001) 221–236.

[16] J.N. Armor, Catalytic removal of nitrogen oxides: where are the opportunities?, Catal. Today. 26 (1995) 99–105.

[17] M. Fu, C. Li, P. Lu, L. Qu, M. Zhang, Y. Zhou, et al., A review on selective catalytic reduction of NO_x by supported catalysts at 100–300°C - catalysts, mechanism, kinetics, Catal. Sci. Technol. 4 (2014) 14–25.

[18] P.K. Hopke, Contemporary threats and air pollution, Atmos. Environ. 43 (2009) 87–93.

[28] S. Bhattacharyya, R.K. Das, Catalytic control of automotive NO_x: A review, Int J Energy Res. 23 (1999) 351–369.

[44] G. Busca, L. Lietti, G. Ramis, F. Berti, Chemical and mechanistic aspects of the selective catalytic reduction of NOx by ammonia over oxide catalysts: A review, Appl. Catal. B Environ. 18 (1998) 1–36.

[45] H. Hamada, M. Haneda, A review of selective catalytic reduction of nitrogen oxides with hydrogen and carbon monoxide, Appl. Catal. A Gen. 421-422 (2012) 1–13.

[46] R. Burch, Low NO_x options in catalytic combustion and emission control, Catal Today. 35 (1997) 27–36.

[57] R. Burch, J.P. Breen, F.C. Meunier, A review of the selective reduction of NO_x with hydrocarbons under lean-burn conditions with non-zeolitic oxide and platinum group metal catalysts, Appl. Catal. B Environ. 39 (2002) 283–303.

[58] J.D. Holladay, J. Hu, D.L. King, Y. Wang, An overview of hydrogen production technologies, Catal. Today. 139 (2009) 244–260.

[59] C.N. Costa, A.M. Efstathiou, Low-temperature H_2-SCR of NO on a novel Pt/MgO-CeO_2 catalyst, Appl. Catal. B Environ. 72 (2007) 240–252.

[60] S. Sharma, S.K. Ghoshal, Hydrogen the future transportation fuel: From production to applications, Renew. Sustain. Energy Rev. 43 (2015) 1151–1158.

[61] M. Mihet, M.D. Lazar, Effect of Pd and Rh promotion on Ni/Al_2O_3 for NO reduction by hydrogen for stationary applications, Chem. Eng. J. 251 (2014) 310–318.

[63] Y. Renème, F. Dhainaut, P. Granger, Kinetics of the NO/H_2/O_2 reactions on natural gas vehicle catalysts-Influence of Rh addition to Pd, Appl. Catal. B Environ. 111-112 (2012) 424–432.

[64] R. Burch, M.D. Coleman, An investigation of the NO/H_2/O_2 reaction on noble-metal catalysts at low temperatures under lean-burn conditions, Appl. Catal. B Environ. 23 (1999) 115–121.

[65] C.N. Costa, P.G. Savva, J.L.G. Fierro, A.M. Efstathiou, Industrial H_2-SCR of NO on a novel Pt/MgO–CeO_2 catalyst, Appl. Catal. B Environ. 75 (2007) 147–156.

[68] P.G. Savva, A.M. Efstathiou, The influence of reaction temperature on the chemical structure and surface concentration of active NO_x in H_2-SCR over Pt/MgO–CeO_2: SSITKA-DRIFTS and transient mass spectrometry studies, J. Catal. 257 (2008) 324–333.

[69] F. Dhainaut, S. Pietrzyk, P. Granger, Kinetic investigation of the NO reduction by H_2 over noble metal based catalysts, Catal. Today. 119 (2007) 94–99.

[70] F. Dhainaut, S. Pietrzyk, P. Granger, NO + H_2 reaction on Pd/Al_2O_3 under lean conditions: kinetic study, Top. Catal. 42-43 (2007) 135–141.

[81] D. Fissore, O.M. Penciu, A. Barresi, SCR of NO_x in loop reactors: Asymptotic model and bifurcational analysis, Chem. Eng. J. 122 (2006) 175–182.

[82] P. Marín, D. Fissore, A. Barresi, S. Ordóñez, Simulation of an industrial-scale process for the SCR of NO_x based on the loop reactor concept, Chem. Eng. Process. Process Intensif. 48 (2009) 311–320.

[83] W. Agar, D.W. Ruppel, Extended reactor concept for dynamic DeNOx design, Chem. Eng. Sci. 43 (1988) 2073–2078.

[84] E. Muñoz, P. Marín, F. V. Díez, S. Ordóñez, Selective catalytic reduction of NO in a reverse-flow reactor: Modelling and experimental validation, Appl. Energy. 138 (2015) 183–192.

[85] C.C. Botar-Jid, P.S. Agachi, D. Fissore, Comparison of reverse flow and counter-current reactors in the case of selective catalytic reduction of NO_x, Comput. Chem. Eng. 33 (2009) 782–787.

[88] R. Zukerman, L. Vradman, M. Herskowitz, E. Liverts, M. Liverts, A. Massner, et al., Modeling and simulation of a smart catalytic converter combining NO_x storage, ammonia production and SCR, Chem. Eng. J. 155 (2009) 419–426.

[92] G. Schaub, D. Unruh, J. Wang, T. Turek, Kinetic analysis of selective catalytic NO_x reduction (SCR) in a catalytic filter, Chem. Eng. Process. 42 (2003) 365–371.

[93] C.-T. Chen, W.-L. Tan, Mathematical modeling, optimal design and control of an SCR reactor for NO_x removal, J. Taiwan Inst. Chem. Eng. 43 (2011) 409–419.

[96] J. Xu, R. Clayton, V. Balakotaiah, M.P. Harold, Experimental and microkinetic modeling of steady-state NO reduction by H_2 on $Pt/BaO/Al_2O_3$ monolith catalysts, Appl. Catal. B Environ. 77 (2008) 395–408.

[97] J. Xu, M.P. Harold, V. Balakotaiah, Microkinetic modeling of steady-state $NO/H_2/O_2$ on $Pt/BaO/Al_2O_3$ NO_x storage and reduction monolith catalysts, Appl. Catal. B Environ. 89 (2009) 73–86.

[102] M. Mihet, M.D. Lazar, V. Almasan, G. Borodi, Low temperature Hydrogen selective catalytic reduction of NO on Pd/Al_2O_3, Rev. Roum. Chim. 56 (2011) 659–665.

[103] M. Mihet, M.D. Lazar, V. Almasan, V. Mirel, H_2-SCR at low temperatures on noble metal supported catalysts, AIP Conf. Proc. 73 (2012) 73–76.

[104] M. Mihet, M.D. Lazar, G. Borodi, V. Almasan, Effect of Pt promotion on Ni/Al_2O_3 for the selective catalytic reduction of NO with hydrogen, AIP Conf. Proc. 126 (2013) 126–132.

[109] G.F. Froment, K.B. Bischoff, J. De Wilde, Chemical Reactor Analysis and Design, third ed., John Wiley & Sons Inc., New-York, 2011.

[122] R. Burch, J.P. Breen, F.C. Meunier, A review of the selective reduction of NO_x with hydrocarbons under lean-burn conditions with non-zeolitic oxide and platinum group metal catalysts, Appl. Catal. B Environ. 39 (2002) 283–303.

[127] M. Mihet, M. Lazar, V. Almasan, Mobility of hydrogen species on Ni supported catalysts, J. Phys. Conf. Ser. 182 (2009) 012051.

[130] P. Granger, J.P. Dacquin, F. Dhainaut, C. Dujardin, The formation of N_2O during NO_x conversion: Fundamental approach and practical developments, in: P. Granger, V.I. Parvulescu (Eds.), Studies in Surface Science and Catalysis, Elsevier, Amsterdam, 171, 2007, pp. 291–324.

[131] M. Gajdoš, J. Hafner, A. Eichler, Ab initio density-functional study of NO on close-packed transition and noble metal surfaces: I. Molecular adsorption, J. Phys. Condens. Matter. 18 (2006) 13–40.

[132] J.Pérez-Ramirez, R.J. Berger, G. Mul, F. Kapteijn, J.A. Moulijn, The six-flow reactor technology A review on fast catalyst screening and kinetic studies, Catal Today. 60 (2000) 93–109.

[161] F.C. Meunier, J. Scalbert, F. Thibault-Starzyk, Unraveling the mechanism of chemical reactions through thermodynamic analyses: A short review, Appl. Catal. A Gen. (2014) 1–8.

[163] F. Dhainaut, S. Pietrzyk, P. Granger, Kinetics of the $NO+H_2$ reaction over supported noble metal based catalysts: Support effect on their adsorption properties, Appl. Catal. B Environ. 70 (2007) 100–110.

[164] A. Kumar, X. Zheng, M.P. Harold, V. Balakotaiah, Microkinetic modeling of the $NO+H_2$ system on Pt/Al_2O_3 catalyst using temporal analysis of products, J. Catal. 279 (2011) 12–26.

[165] R.J. Berger, F. Kapteijn, J.A. Moulijn, G.B. Marin, J. De Wilde, M. Olea, et al., Dynamic methods for catalytic kinetics, Appl. Catal. A Gen. 342 (2008) 3–28.

[168] Comsol Multiphysics User's Guide, Version 4., COMSOL AB, 2010.